Article:
Ševo, B., Bašić, A., Amdursky, N. et al. (2026) Recent advances in biopolymer-based membranes for proton exchange membrane fuel cells. Energies, 19 (10). 2426. ISSN: 1996-1073

https://doi.org/10.3390/en19102426

energies

MDPI

Review

Recent Advances in Biopolymer-Based Membranes for Proton Exchange Membrane Fuel Cells

Bruno Ševo [1], Anita Bašić [2], Nadav Amdursky [3,4] and Željko Penga [1,*]

[1] Faculty of Electrical Engineering, Mechanical Engineering and Naval Architecture University of Split, R. Boškovića 32, 21000 Split, Croatia; bsevo00@fesb.hr
[2] Department of Chemical Engineering, Faculty of Chemistry and Technology, University of Split, Ruđera Boškovića 35, 21000 Split, Croatia; abasic@ktf-split.hr
[3] Schulich Faculty of Chemistry, Technion—Israel Institute of Technology, Haifa 3200003, Israel; amdursky@technion.ac.il or n.amdursky@sheffield.ac.uk
[4] Chemistry, School of Mathematical and Physical Sciences, University of Sheffield, Sheffield S3 7HF, UK
* Correspondence: zpenga@fesb.hr; Tel.: +385-91-4305 958

Abstract

Proton exchange membrane fuel cells (PEMFCs) are among the most promising clean energy conversion technologies, offering high efficiency and zero emissions. However, their large-scale commercialisation is limited by the high cost and environmental impact of conventional perfluorosulfonic acid membranes such as Nafion. In recent years, increasing attention has been directed toward biopolymer-based membranes as sustainable, low-cost, and biodegradable alternatives. This review provides a comprehensive overview of recent advances in the development and modification of biopolymer membranes, including polysaccharide-based materials such as chitosan, cellulose, gellan gum, sodium alginate, and starch, as well as protein-based materials such as keratin and collagen. Various modification strategies, including sulfonation, phosphorylation, cross-linking, and incorporation of inorganic or hybrid fillers, are analysed for their impact on key parameters, including proton conductivity, methanol permeability, and power density. Comparative data indicate that several modified biopolymer membranes achieve proton conductivities of 50 mS/cm or higher. However, higher conductivity values are generally reported for membranes primarily composed of synthetic polymers, where the biopolymer is incorporated only as an additive. In addition, some biopolymer-based membranes exhibit significantly lower methanol permeability than Nafion. The lowest reported value among the membranes discussed in this article is 0.98×10^{-16}, representing the best-performing biopolymer membrane in terms of methanol permeability alone. Although many biopolymer membranes demonstrate relatively poor performance in single PEMFC tests, several have achieved power densities comparable to Nafion, while simultaneously offering improved environmental compatibility and sustainability. Finally, current challenges and future directions are discussed, emphasising the potential of these renewable materials to advance PEMFC technology toward more sustainable and economically viable energy systems.

Keywords: PEM fuel cell; biopolymer; membrane; cellulose; chitosan; biodegradable; sulfonation; crosslink; phosphorylation; proton conductivity

Academic Editor: Felix Barreras

Received: 17 February 2026
Revised: 23 March 2026
Accepted: 14 May 2026
Published: 18 May 2026

1. Introduction

Energy plays a key role in modern society, enabling economic growth, technological progress, and the provision of basic services. However, the ever-increasing world popu-

lation, estimated to be around 8.2 billion in 2025, and rising energy demand are placing additional strain on existing energy systems. For more than a century, fossil fuels have been the dominant energy source, but their limited availability and serious environmental consequences, including global warming, sea level rise, and extreme weather events, pose major challenges. Estimates indicate that fossil fuel reserves could be exhausted in 60–80 years if current consumption levels continue [1]. In addition to its depletion, burning of fossil fuels emits large amounts of CO_2 and other greenhouse gases, further exacerbating climate change [2]. Given these challenges, the scientific community and policymakers increasingly recognise the need to transition from fossil fuel-based energy systems to renewable, clean, and sustainable energy sources. In this context, alternative energy solutions, including renewable sources such as solar, wind, hydropower, geothermal, and bioenergy, are being increasingly researched [3]. Due to inherent limitations in the intermittent and fluctuating nature of natural resources, their stability in energy supply has been limited. In contrast to fossil fuels, which occur naturally and are readily available, hydrogen is not found in significant quantities in its free form and therefore needs to be produced from other energy sources. Hydrogen energy holds significant potential in clean energy transition and is an effective pathway for achieving large-scale deep decarbonization. The electrolysis of water for green hydrogen production is not only one of the ways to obtain hydrogen energy, but also contributes to addressing the intermittency and variability of renewable energy sources [4]. Furthermore, hydrogen can be utilised in technologies such as fuel cells to generate electricity with water as the only by-product, highlighting its role as a clean and environmentally sustainable energy carrier [5]. This energy transition not only addresses the challenges of fossil fuel depletion but also helps mitigate negative environmental impacts, ensuring a more sustainable energy future.

Fuel cells are electrochemical devices that convert chemical energy into electricity through redox reactions. Unlike conventional batteries, fuel cells can operate continuously as long as the fuel supply is maintained, which is why they are used in a wide range of applications, from portable devices to stationary energy sources, and increasingly in transport. Automobile companies such as Toyota, Honda, and Hyundai have already launched electric vehicles powered by fuel cells on the market [6]. However, interest is increasingly shifting from light vehicles to applications in heavy transport such as trucks, buses, locomotives, and maritime traffic, where the high gravimetric energy density of hydrogen can be better utilised [7]. Fuel cells are classified according to operating temperature (low-temperature, medium-temperature, and high-temperature) or the type of electrolyte, with proton exchange membrane fuel cells (PEMFCs) being particularly prominent due to their advantages, such as low operating temperature (<80 °C), fast response, low mass, and high specific power density [8]. One of the primary challenges associated with PEMFCs is the degradation and limited durability of the membrane–electrode assembly (MEA). As reported by Meng et al. [9], fuel cells typically experience a gradual performance decline during prolonged operation. This degradation results from multiple interacting mechanisms, including catalyst dissolution and agglomeration, corrosion of electrode materials, mechanical and chemical degradation of the MEA, and variations in operating conditions such as temperature, humidity, and load cycling. Consequently, performance loss reduces fuel cell efficiency and power output, while shortening operational lifetime and increasing maintenance and replacement costs.

The core of an MEA and a PEMFC is the proton exchange membrane (PEM), which accounts for 30% of the material cost of the entire fuel cell [6]. The membrane performs three key functions within the fuel cell: (1) it enables the transport of protons from the anode to the cathode, (2) it forces electrons to travel through the external circuit (i.e., it provides high electrical resistance), and (3) it separates the reactants. The proper functioning of

the membrane requires several material properties such as high proton conductivity, low electronic conductivity, low fuel permeability, and chemical, thermal, and mechanical stability [10].

Commercial membranes can meet most of the above requirements to serve as efficient membranes for fuel cell systems [11]. However, their high cost limits the wider application of PEMFCs. By comparison, PFSA resin dispersion produced in Dongyue, Shandong, China, costs approximately USD 500 per litre. Preparing a 10 × 10 cm membrane with a thickness of 25 μm requires about 10 mL of this dispersion, corresponding to a material cost of roughly USD 5. Including additional experimental consumables, the total cost remains below USD 10. In contrast, a commercially available Nafion membrane of the same size and thickness costs around USD 30, which is significantly higher than that of membranes fabricated from Dongyue PFSA dispersion [12]. In addition to high cost, the tightening of environmental regulations in many countries (e.g., Japan and Germany) is directing research and development towards the production of membranes from non-polluting materials using sustainable techniques and processes [13]. This trend has stimulated considerable interest in the search for biodegradable materials that are not based on petroleum derivatives [14].

In recent years, significant attention has been devoted to developing new types of membranes based on biopolymers, as biopolymers are inexpensive, readily available, and possess effective intrinsic properties [15]. In particular, cellulose (microcrystalline/nanocrystalline cellulose, cellulose nanofibres, bacterial cellulose, and their derivatives) and chitosan are being investigated as potential materials for membranes in PEMFCs. Figure 1 shows the continuous and rapid increase in the number of scientific publications on ion exchange membrane fuel cells (IEMFCs) from 2001 to 2020. The blue columns indicate the total number of publications per year, while the green columns, obtained from additional searches using the keywords 'cellulose', 'chitosan', or 'biopolymer', show the number of papers on biopolymeric membranes for ion exchange. It is clear that synthetic polymer membranes remain the primary focus of research, while biopolymer membranes are underrepresented in scientific studies. One of the reasons for this may be that biopolymer membranes are still in the early stages of research, and, consequently, many researchers are not yet familiar with this topic. In contrast, synthetic polymers are well-established in the PEMFC community, so most studies focus on their properties and performance.

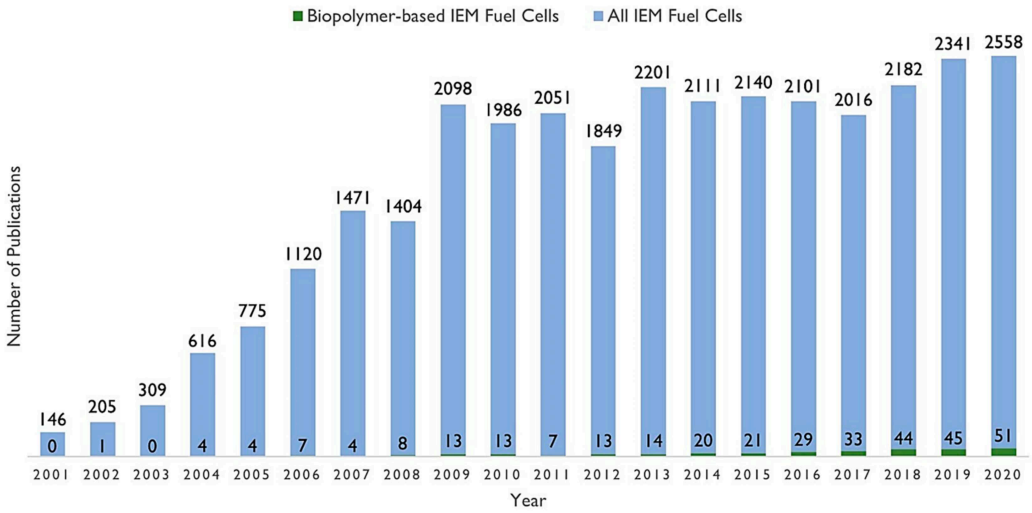

Figure 1. Number of scientific publications related to IEMs based on synthetic polymers compared to IEMs based on biopolymers from 2001 to 2020 [16].

Recent review articles on biopolymer membranes have predominantly focused on a single class of materials, such as cellulose-based membranes [17] or chitosan-based membranes [18]. Although a few studies have addressed both cellulose and chitosan-based membranes within the same review [16,19], the internal classification of these materials is often unclear, and the discussion typically emphasises one biopolymer while providing only limited coverage of the other. To the best of our knowledge, no comprehensive review has systematically examined biopolymer membranes from a broader perspective that includes both polysaccharide-based and protein-based membranes within a unified framework.

In the present review, commonly investigated polysaccharide-based membranes, particularly cellulose and chitosan, are clearly categorised into distinct subsections to facilitate better comparison and structural clarity. This organisation enables readers to more easily identify the classification and characteristics of each reported membrane. Furthermore, all membranes discussed in this article are evaluated from a mechanical engineering perspective, with particular emphasis on proton conductivity and the polarisation curves of the tested membranes. The curve reflects several factors including activation, ohmic, and concentration polarisation losses [20], and is a key parameter for assessing membrane performance. However, it only describes the steady-state voltage properties, so durability testing is also essential to properly evaluate membrane performance in PEMFCs. Most membranes in the literature have not undergone long-term durability tests and those that have were typically only measured for a few hours, which is insufficient to evaluate long-term operational stability.

Finally, this review compares and analyses how different biopolymer compositions and modification techniques influence different membrane properties, thereby determining their suitability and potential for improving the overall efficiency and sustainability of PEMFC technology.

2. Biopolymers

The high cost and environmental drawbacks of conventional synthetic polymer membranes, such as toxic production processes and slow biodegradation, have increased interest in biopolymer-based alternatives for PEMFCs. Biopolymers offer a more sustainable and environmentally friendly solution due to their natural origin, rapid biodegradability, and lower environmental impact. These materials are generally categorised into two main groups based on their chemical composition and source. The first group consists of polysaccharide-based biopolymers, including chitosan, cellulose, gellan gum, sodium alginate, and starch, which are derived from plant or marine sources and known for their excellent film-forming ability and chemical versatility. The second group comprises protein-based biopolymers, such as keratin and collagen, which possess unique mechanical properties and functional groups that can facilitate proton transport when properly modified or blended with other materials. Moisture content critically governs proton conductivity in PEMs by mediating dual transport mechanisms: (i) the vehicular mechanism and (ii) the Grotthuss hopping mechanism as reported in [21].

The vehicular mechanism refers to proton transport via water molecules that act as "vehicles" forming hydrated ions such as H_3O^+, $H_5O_2^+$, and $H_9O_4^+$, which diffuse along concentration gradient [22].

The Grotthuss hopping mechanism involves the transfer of protons through a hydrogen-bonded network without the physical movement of the molecule's enabling rapid proton transport [23].

A schematic of both mechanisms for most widely used PEM Nafion, without and with fillers, is shown in Figure 2. In hybrid membranes, proton conductivity also depends on the chemical properties and the interface between organic and inorganic phases [24].

Furthermore, chemical modifications, such as sulfonation (–SO_3H) and phosphorylation, enhance proton transport by increasing hydrophilicity and facilitating both vehicular and Grotthuss mechanisms.

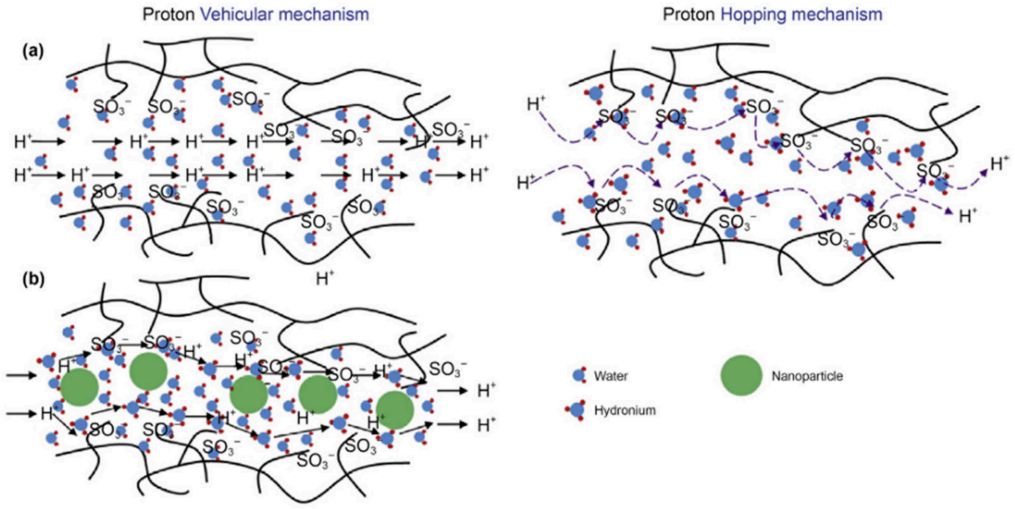

Figure 2. Schematic representation of the vehicle mechanism and the Grotthuss hopping mechanism in (**a**) polymer membranes and (**b**) polymer–nanoparticle composite membranes [25].

2.1. Chitosan

Chitosan (CS) is one of the most abundant polysaccharides in nature. It is obtained by the deacetylation of chitin, which can be extracted from various sources, such as mould cell walls, silkworms, and the shells of shrimps, crabs, cockroaches, lobsters, and wings [26]. CS has a high affinity for water due to the presence of three functional groups, as shown in Figure 3: hydroxyl (–OH), primary amine (–NH_2), and C-O-C groups. The presence of hydrogen bonds in the (–OH and –NH_2) functional groups accounts for the rigid, highly crystalline structure of chitosan. Additionally, the amine group makes chitosan more reactive than cellulose. In addition to its high affinity for water, CS is biodegradable, biocompatible, non-toxic, and inexpensive. These properties have encouraged the use of CS as a cheap, environmentally friendly PEM since 2003, particularly CS with a high molar mass (>150,000 g/mol) and a low degree of deacetylation (<70%). This enables higher proton conductivity, on the order of 100 mS/cm, compared to chitosan with a low molar mass (<150,000 g/mol) and a higher degree of deacetylation (>70%) [27]. However, CS cannot be used directly as a PEM due to its low proton conductivity, resulting from the absence of a mobile proton in its structure and physicochemical properties that are unreliable for the durability of PEMFCs [28]. The use of synthesis and modification techniques plays a key role in improving the properties of chitosan. Various methods have been investigated to enhance the characteristics of chitosan, including chemical modifications, blending with organic–inorganic hybrids, doping with inorganic fillers, and producing nanocomposites.

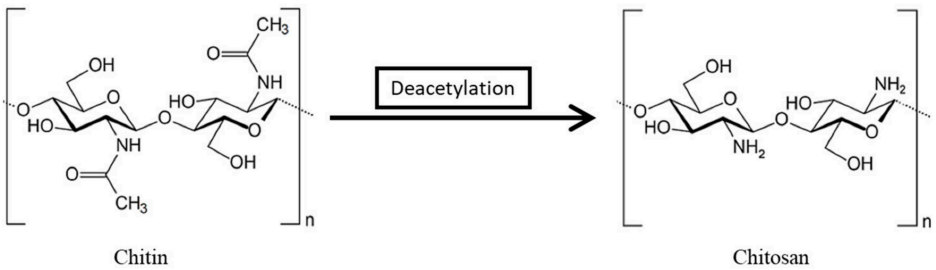

Figure 3. Structure of chitin and chitosan [19].

2.1.1. Chemical Modifications of Chitosan

The process of chemical modification involves incorporating functional groups into the molecular structure of chitosan to improve its properties through sulfonation or phosphorylation, depending on which acid group is incorporated into the polymer backbone. Chemical modification, particularly by cross-linking polymer chains, can increase the proton conductivity and mechanical strength of chitosan [29].

- Sulfonation

The sulfonation of chitosan entails the incorporation of sulfonic acid groups (–SO_3H) into the polymer backbone, a modification that significantly improves both mechanical robustness and proton conductivity. This chemical alteration is pivotal for tailoring the biopolymer for fuel cell environments, where high ionic transport is required. The fundamental steps and structural changes in the sulfonation of chitosan are illustrated in the schematic in Figure 4. Introducing these acidic functional groups, the hydrophilic nature of the membrane is typically enhanced, facilitating a more efficient proton conduction pathway through the polymer matrix. Sulfonation can be performed in two ways: by attaching (–SO_3H) groups to an amino group (–NH_2) or to a hydroxyl group (–OH), resulting in different functional derivatives. The correct level of sulfonation is crucial, as insufficient sulfonation leads to low ionic conductivity and weaker ion exchange, while excessive sulfonation can reduce mechanical strength and cause excessive water absorption, negatively impacting membrane stability and durability [30,31]. The optimal level of sulfonation achieves a balance between ion exchange, proton conductivity, mechanical strength, water absorption, and methanol permeability.

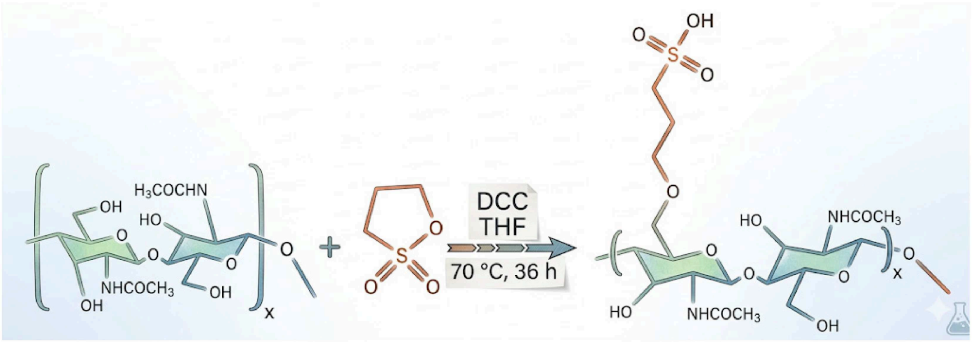

Figure 4. Sulfonation of chitin nanofibres.

Kalaiselvimary and Prabhu [32] developed nanocomposite membranes based on sulfonated chitosan (s-CS), polyethylene oxide (PEO), and sulfonated graphene oxide (s-GO) for use in fuel cells. Research has shown that the optimal filler content is 6 wt% s-GO, at which ionic conductivity reaches approximately 100 mS/cm. A higher amount of s-GO (>6 wt%) led to decreased conductivity due to ion channel blocking and filler aggregation. Additionally, sulfonation and the optimal dispersion of s-GO significantly improved thermal stability, interfacial compatibility, and ion exchange capacity.

Nasirinezhad et al. [33] also demonstrated the importance of sulfonation as an effective method for increasing the proton conductivity of biopolymer membranes for direct methanol fuel cells (DMFCs). Sulfonated chitin nanofibres (sChW) were introduced as functional fillers into the chitosan matrix, creating additional pathways for proton conduction through –SO_3H groups. The optimal amount of sChW was 5 wt%, at which the best balance between high proton conductivity (12.1 mS/cm) and low methanol permeability (4.5×10^{-7} cm^2/s) was achieved. This combination resulted in a membrane selectivity of 26,888 Ss/cm^3, about 6.8 times higher than that of the pure chitosan membrane. Exceeding the optimal filler concentration (e.g., 7 wt%) led to nanofibre agglomeration and

increased methanol permeability. The results show that functionalising the nanofillers with sulfonation is essential for efficient proton conduction and for reducing unwanted methanol permeability, making these membranes suitable for use in DMFC systems.

- Phosphorylation

Phosphorylation of chitosan involves incorporating phosphoric acid groups ($–PO_3H_2$) into its structure, increasing the number of acidic functional groups that facilitate proton binding and transfer. This significantly enhances proton conductivity, which is essential for the efficient operation of membranes in fuel cells [34]. The phosphoric acid functional group is widely regarded as a highly effective proton conductor, surpassing many other acidic groups due to its efficient proton solvation, strong self-ionisation, and extensive intermolecular hydrogen-bonding network [35]. Its lower proton dissociation energy (37.2 kJ mol^{-1}) compared with that of the sulfonic acid group (69.9 kJ mol^{-1}) facilitates easier proton migration through acid–acid interactions [36]. In addition, phosphoric acid exhibits a higher affinity for water, with a binding energy of 47.3 kJ mol^{-1} compared with 44.4 kJ mol^{-1} for sulfonic acid, contributing to enhanced water retention within the membrane. Phosphoric acid functionality can be incorporated into membranes through several approaches: (1) the impregnation of polymer matrices with liquid phosphoric acid, (2) chemical attachment of phosphoric acid groups to polymer backbones, and (3) the grafting of phosphoric acid groups onto inorganic nanofillers [37,38].

Ahmed et al. [39] phosphorylated graphene oxide (GO) using aminotris (methylenephosphonic acid) (ATMP) to produce phosphorylated graphene oxide (PGO) with enhanced properties for PEMFC applications. The phosphorylation was performed in a single step, making the process simple and efficient. The optimal PGO content in the chitosan-based composite membrane was 2 wt%, resulting in a proton conductivity of 36 mS/cm, which is higher than that of the commercial Nafion 117 membrane (33 mS/cm). Additionally, PGO improved the thermal and mechanical stability of the membrane through strong electrostatic and hydrogen bonding between the functional groups of GO and chitosan. Ahmed et al. [40] used the same phosphorylation procedure, but employed functional multi-walled carbon nanotubes (N-MWCNTs) instead of graphene oxide as a filler in a phosphorylated chitosan matrix (PCS). The optimal filler content was 5 wt% N-MWCNTs, resulting in the highest proton conductivity of 45 mS/cm at 80 °C, as well as improved mechanical and thermal properties of the membrane. This composite membrane showed significant oxidation stability (degradation time of 148 min in Fenton's reagent) and dimensional stability. In practical tests within a hydrogen fuel cell, the PCS/N-MWCNT membrane with 5 wt% filler achieved a maximum power density of 49.75 mW/cm^2, nearly double that of PCS without filler (27.31 mW/cm^2), as can be seen in Figure 5. These two studies confirm the importance of phosphorylation and the optimal amount of functional filler for the effective application of biopolymer membranes in PEMFC systems.

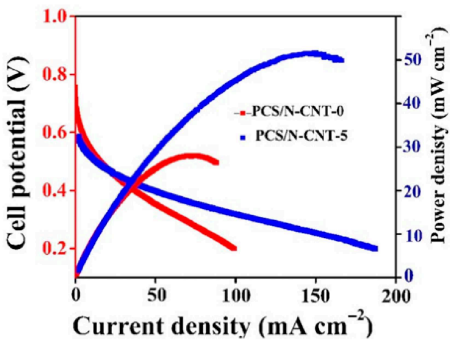

Figure 5. Polarisation curves and power density curves of single fuel cells at 50 °C (reprinted with permission from Ref. [40]. Copyright (2023) IOP Science).

- Cross-linking

Cross-linking enhances the stability, mechanical strength, and functionality of chitosan by forming a network structure [41]. This process involves adding cross-linking agents, such as glutaraldehyde, epichlorohydrin, or sulphuric acid, which interact with the amino groups of chitosan to form durable covalent bonds.

Handika et al. [42] investigated the synthesis of a composite membrane based on chitosan and fly ash for fuel cell applications. The membrane was cross-linked with sulphuric acid, which improved its structural stability and proton conductivity. The optimal fly ash concentration was 10 wt%, at which the membrane achieved the highest proton conductivity of 6.863 mS/cm. The addition of fly ash also reduced methanol permeability, with the lowest value of 2.85×10^{-6} cm^2/s observed for the membrane containing 15 wt% filler.

Vijayakumar and Khastgir [43] investigated hybrid composite membranes based on chitosan, sulfonated polyaniline (PAni), and silica (SiO_2) for DMFC applications. The membrane was cross-linked with sulphuric acid, which improved its mechanical strength and oxidative stability. The optimal concentration of the PAni/SiO_2 filler was 3 wt%, at which the membrane achieved the highest proton conductivity of 8.39 mS/cm at 80 °C, due to the formation of hydrophilic domains and additional pathways for proton conduction. Single fuel cell tests showed that the membrane with 3 wt% filler had the highest power density of 56.27 mW/cm^2, significantly higher than that of the pure chitosan membrane (41.15 mW/cm^2). The addition of filler reduced methanol permeability, but an excessive concentration (e.g., 7 wt%) led to particle aggregation and decreased conductivity.

2.1.2. Addition of Inorganic Fillers

Adding inorganic fillers to chitosan membranes for fuel cells is an effective way to improve their physicochemical properties. Fillers, such as graphene oxide or nanotubes, improve mechanical strength, thermal stability, proton conductivity, and chemical resistance. They may be incorporated in situ within the matrix or mixed with the polymer before casting the membrane. The functionalisation of fillers, for example, by sulfonation, further increases conductivity by providing additional sites for proton transfer. However, compatibility between chitosan and the filler remains a challenge, which can be evaluated using the Flory–Huggins interaction parameter. Compatibility can be improved by chemical modification of the filler or chitosan, ensuring better dispersion and interfacial adhesion [44,45].

- Heteropoly acids

Heteropoly acids (HPAs), such as phosphotungstic acid (PTA), phosphomolybdic acid (PMA), and silicotungstic acid (SiWA), are an important group of proton-conducting materials. Because of their outstanding superionic conductivity, these acids have received significant attention and have been extensively explored for PEM applications [46]. In particular, PTA, which has a well-defined Keggin structure, is a promising candidate for enhancing membrane efficiency. Despite these advantages, HPAs often suffer from excessive water uptake and gradual leaching, both of which compromise long-term fuel cell performance. To mitigate this, researchers have promoted electrostatic interactions between the polymer matrix and HPA species to improve retention and stability. Building on this approach to address the critical challenge of phosphoric acid leaching, recent studies have successfully incorporated amino-functionalized porous aromatic frameworks (PAF-20-NH_2) into PBI membranes. The integration of these advanced fillers not only yields high proton conductivity but also ensures superior high-temperature stability, representing a vital breakthrough for the advancement of high-temperature PEMFCs [47].

Tsen [48] investigated composite PEMs based on chitosan and PTA immobilised on one-dimensional attapulgite (AT) for use in DMFCs. PTA, a strong heteropoly acid and an excellent proton conductor, was used to improve the proton conductivity and mechanical properties of the membranes. The composite membrane with 4 wt% PTA-AT showed a proton conductivity of 35.3 mS/cm at 80 °C, which was 31.8% higher than that of the pure chitosan membrane. In addition, the membrane reduced methanol permeability and achieved a maximum power density of 70.26 mW/cm^2 at 2 M methanol, significantly higher than the 40.08 mW/cm^2 of the pure chitosan membrane. The polarisation and power density curves of the DMFC tests are presented in Figure 6. These results confirm that PTA contributes to the formation of efficient proton transport channels, making composite membranes promising candidates for DMFC applications.

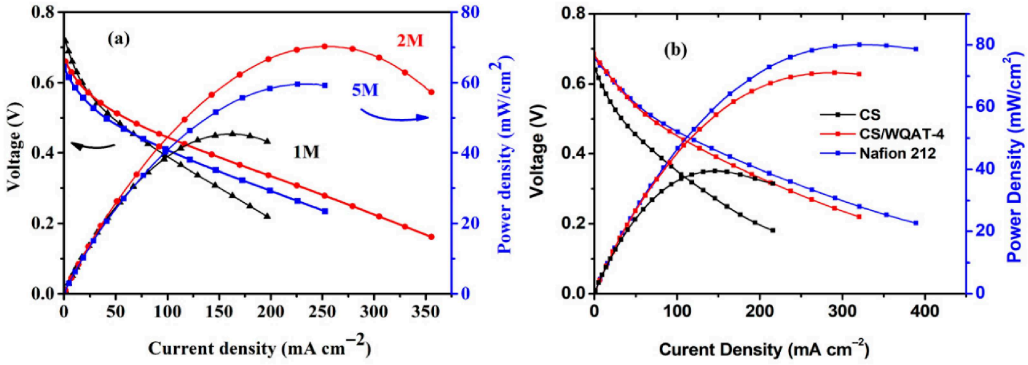

Figure 6. Polarisation curves and power density curves of DMFC tests with (**a**) CS/WQAT-4 composite membrane at different methanol concentrations, and (**b**) different PEMs at 70 °C with 2M methanol [48].

Zaffora et al. [49] also fabricated composite membranes based on chitosan and PTA for use in DMFCs. The membranes were prepared by ionotropic gelation, with PTA used as a heteropoly acid to improve proton conductivity. The results showed that membranes with higher PTA content exhibited improved proton conductivity, reaching 12 mS/cm at 70 °C. The fuel cell using these membranes achieved a maximum power density of 60 mW/cm^2 at a low methanol concentration (1 M) and low catalyst concentration (0.5 mgPt/cm^2 at the cathode and 3 mgPt/cm^2 Pt-Ru at the anode). Additionally, the membranes demonstrated low methanol permeability with a diffusivity of 3.6 × 10^{-6} cm^2/s, comparable to commercial Nafion membranes.

Di Franco et al. [50] developed composite membranes based on chitosan and SiWA and investigated their performance in a fuel cell using hydrogen and oxygen at room temperature. The results showed that the membrane functions effectively as a proton conductor and that the duration of functionalisation significantly affects its performance. Specifically, without functionalisation, the membrane showed no proton conduction, whereas 24 h functionalisation resulted in a maximum power density of 268 mW/cm^2 at 0.5 mgPt/cm^2, or 370 mW/cm^2 at 1 mgPt/cm^2. Prolonged functionalisation also led to a decrease in internal membrane resistance and increased proton conductivity (up to 4.88 mS/cm). Tafel and electrochemical impedance spectroscopy (EIS) analyses indicated improved oxygen reduction kinetics and a stable electrode–electrolyte interface. It was found that a longer cross-linking and functionalisation period led to a better membrane arrangement, which further improved its efficiency in PEMFC systems. This study highlights the importance of optimising synthesis conditions to achieve the improved performance of chitosan membranes.

- Hygroscopic oxides

The addition of hygroscopic oxides to the chitosan matrix significantly improves the properties of PEMs. These oxides, such as TiO_2, SiO_2, ZrO_2, zeolite, and montmorillonite, improve membrane hydration, which is essential for efficient proton transfer and the prevention of membrane dehydration [51]. Modification of these fillers, for example, by sulfonation or the addition of carboxyl groups, further increases proton conductivity and reduces methanol permeability. Composite membranes with functional zeolites and silica show higher thermal and mechanical stability and improved resistance to methanol [52]. Such hybrid materials are promising, environmentally friendly electrolytes for use in PEM fuel cells.

Shang et al. [53] investigated the effect of incorporating hygroscopic silicon oxide (SiO_2) in a core–shell structure into the chitosan matrix to improve the performance of PEMs for DMFC applications. Hygroscopic SiO_2 was synthesised by emulsion polymerisation without emulsifiers, ensuring homogeneous distribution and preventing nanoparticle agglomeration. The membranes were further cross-linked with sulphuric acid to increase mechanical stability and create additional pathways for proton conduction. The optimal chitosan content was 10 wt%, achieving the best balance between proton conductivity (12.4 mS/cm) and very low methanol diffusion (on the order of 10^{-8} cm^2/s), with selectivity 11.6 times higher than that of the Nafion 117 membrane. Compared to commercial PEMs, these membranes exhibit excellent methanol barrier properties, good conductivity, and mechanical strength, making them suitable candidates for DMFCs.

Gómez et al. [54] also investigated the effect of adding hygroscopic oxides, specifically titanium dioxide (TiO_2) nanoparticles, to a polymer matrix based on chitosan and polyvinyl alcohol (PVA). The membranes were produced by solution casting, with TiO_2 added in concentrations ranging from 0.10 to 5 wt%. It was shown that a low filler concentration (0.10 wt%) enables high moisture absorption (up to 90%), which promotes ionic conductivity, whereas higher concentrations reduce hydration capacity due to pore closure and decreased free volume. The optimal filler amount resulted in balanced thermal, mechanical, and ionic properties. The membrane showed increased ionic conductivity after doping with 4 M KOH, with reduced activation energy (0.38 eV), indicating more efficient ion transfer. In a PEM fuel cell, this doped membrane achieved an open-circuit voltage of 1.0 V, comparable to that of commercial Nafion 117 under high humidity (95% relative humidity) conditions.

- Metal–organic frameworks

Metal–organic frameworks (MOFs) are important materials for producing PEMs, which are essential in fuel cell technology. Their porous structure, large specific surface area, and tunable chemical properties enable efficient proton transport, enhancing the conversion of chemical energy into electrical energy [55]. Doping MOFs into the chitosan matrix can improve proton conductivity, thermal stability, and chemical resistance, thereby increasing the efficiency and durability of PEMs. However, challenges remain. MOFs can lose structural stability under humid and high-temperature fuel cell operating conditions, leading to structural degradation. Additionally, synthesising MOFs with precise pores and functional groups can be technically challenging and costly. There is also a risk of MOF leaching, which can cause electrolyte fouling and reduce membrane performance. The incorporation of MOFs requires advanced manufacturing methods to ensure uniform distribution and good contact with the electrodes, further complicating their application [56].

The influence of adding MOFs, specifically SO_3H-UiO-66, to the DMFC performance of chitosan membranes was investigated by Zhao et al. [57]. MOFs were deposited on the surface of halloysite nanotubes (HNTs) using a simple in situ method, creating core–shell nanohybrids with high dispersibility in a chitosan matrix. The addition of 10 wt% SO_3H-

UiO-66@HNTs resulted in the best overall performance, whereby proton conductivity reached 46.2 mS/cm at 80 °C, and power density in the DMFC was 84.5 mW/cm^2 at 70 °C, which is 77.1% higher than that of the pure CS membrane. The optimal filler amount also reduced methanol permeability by 54.1%, increased membrane selectivity, and improved mechanical strength by 73.5%. In addition, the membrane showed better long-term stability and a lower open-circuit voltage drop compared to commercial Nafion 115. These results confirm that the homogeneous dispersion and functionality of MOFs significantly enhance PEM performance for DMFC applications.

- Carbon nanotubes

Carbon nanotubes (CNTs), often referred to as buckytubes, represent a class of cylindrical nanostructures composed entirely from carbon atoms. These materials are generally classified into two main types based on their structural configuration: single-walled carbon nanotubes (SWCNTs) and multi-walled carbon nanotubes (MWCNTs). The difference between these types is in the number of concentric graphitic layers. SWCNTs consist of a solitary atomic layer of carbon, while MWCNTs contain several nested layers. This structural variation is a crucial factor, as it significantly influences the physical properties of the nanotubes and their subsequent suitability for specific technological applications, such as reinforcing biopolymer electrolyte matrices. CNTs exhibit high mechanical strength and unique electrical and thermal properties, making them suitable for use in advanced materials and devices. However, their application in PEMs is limited by their electrical conductivity, which can cause short circuits, and their tendency to agglomerate, making even distribution in the polymer matrix difficult. Solutions include functionalising CNTs by sulfonation, carboxylation, oxidation, or polymer attachment to improve their dispersibility and compatibility with polymers [58].

Ahmed et al. [59] investigated the role of multi-walled carbon nanotubes (MWCNTs) functionalised with sulfonic acid groups in improving the properties of chitosan membranes for fuel cell applications. MWCNTs were sulfonated by two methods, using 1,3-propane sultane (PS method) and distillation–precipitation polymerisation (DP method), which is later incorporated into the chitosan matrix. The optimal filler amount was 5 wt%, at which the membranes showed the highest proton conductivity of 26 mS/cm (PS@CNT) and 25 mS/cm (DP@CNT), along with improved mechanical and thermal properties. Sulfonic acid groups on the surface of MWCNTs enabled the formation of acid–base pairs with the -NH_2 groups of chitosan, thus creating continuous transmission channels for protons. The addition of CNTs also improved tensile strength and reduced swelling, thereby increasing the dimensional stability of the membrane. Although the conductivity is lower than that of Nafion 117, CS/MWCNT membranes represent a viable and efficient alternative for PEM fuel cells due to their simple preparation process and significant overall performance improvement.

The importance of incorporating MWCNTs into the chitosan matrix to improve membrane performance in DMFCs was also demonstrated by Murmu et al. [60]. CNTs were added at concentrations ranging from 0.5 to 2 wt%, and the membranes were further functionalised with ionic liquid (IL) to improve filler dispersion and ionic conductivity. The optimal CNT content was 1.5 wt% (with IL), at which the CPCN@IL-3 membrane showed the highest proton conductivity of 2.152 mS/cm at 70 °C and the highest selectivity (1.92×10^4 Ss/cm^3). This membrane also showed low methanol permeability (7.26×10^{-8} cm^2/s) and high stability in fuel cell operating conditions. The addition of CNTs reduced methanol permeability and improved mechanical and thermal properties, while IL further increased ion exchange capacity and water binding capacity. In practical tests, the CPCN@IL-3 membrane achieved better performance, as shown in Figure 7.

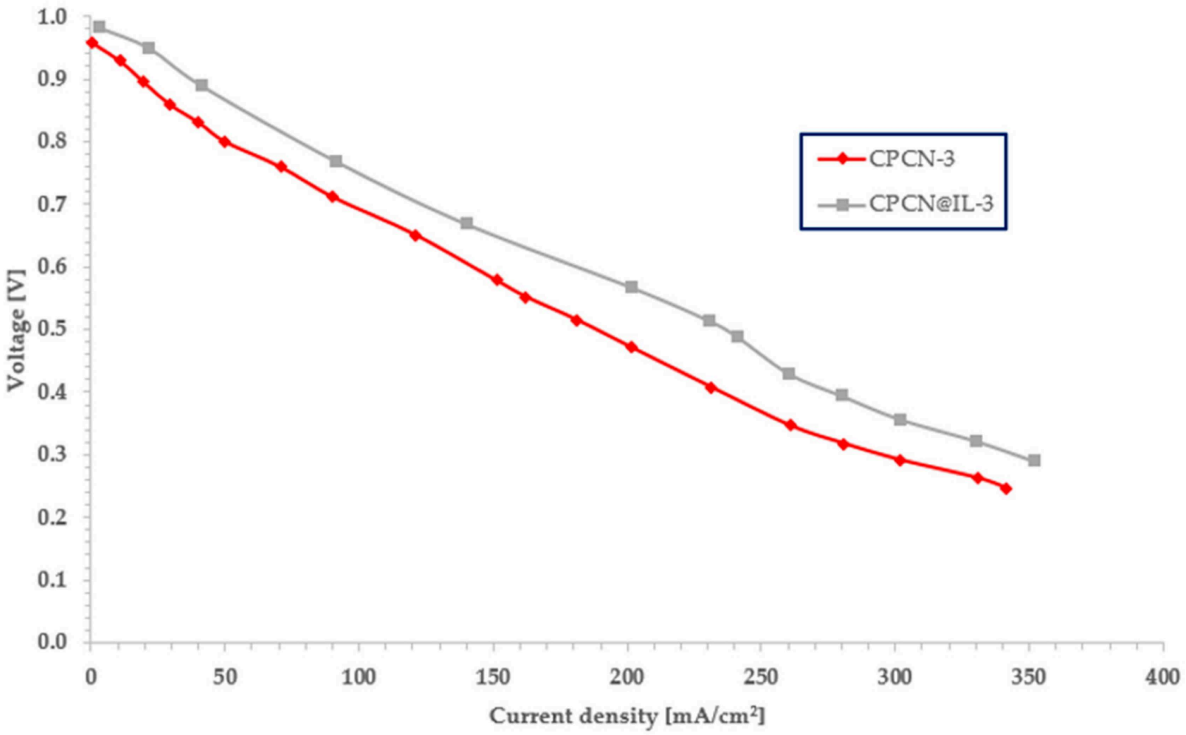

Figure 7. Polarisation curves of CPCN-3 and CPCN@IL-3 membranes at 70 °C and 2M methanol concentration, based on data from [60].

2.2. Cellulose

Cellulose $(C_6H_{10}O_5)_n$, the most abundant naturally occurring polysaccharide, consists of long chains of D-glucose units through β(1→4) glycosidic bonds. Although plants are the primary source, certain microorganisms, including bacteria and fungi, also synthesise cellulose. Its structural organisation typically includes both crystalline and amorphous regions, with their relative proportions depending on factors such as chain length and degree of polymerisation. The crystallinity of cellulose generally ranges between 40 and 70%, varying with the source material and extraction technique employed. Physical, chemical, and enzymatic treatments largely preserve the crystalline regions, while the less ordered, low-density amorphous domains are more susceptible to interactions with other molecular species. Variations in molecular orientation, van der Waals forces, intra- and intermolecular interactions, as well as processing and extraction conditions, give rise to multiple cellulose polymorphs, including cellulose I, II, III_1, III_2, IV_1, and IV_{11}. These polymorphic forms can be transformed into one another through appropriate chemical or thermal treatments [61]. The extensive hydrogen-bonding network within cellulose underpins its high structural stability and restricts its solubility to a limited range of solvents. Based on differences in structure, morphology, and molecular arrangement, cellulose is commonly categorised as microcrystalline cellulose (MCC), nanocrystalline cellulose (CNC), cellulose nanofibres (CNFs), also known as nanofibrillated cellulose, bacterial cellulose (BC), and various cellulose derivatives, such as cellulose acetate (CA) [62].

2.2.1. Micro/Nanocrystalline Cellulose

Cellulose from plant or bacterial sources can undergo acid hydrolysis, which preferentially removes the amorphous regions, enriching the crystalline fraction and the formation of microcrystalline cellulose (MCC). Further processing of MCC yields nanocrystalline cellulose (CNC), as illustrated in Figure 8. CNC particles typically exhibit a rod-like morphology with lengths of approximately 50–200 nm. When dispersed in polymer matrices, CNC leads to improved mechanical properties such as stiffness, tensile strength, and flexural strength, and its surface chemistry enables further chemical functionalisation [63].

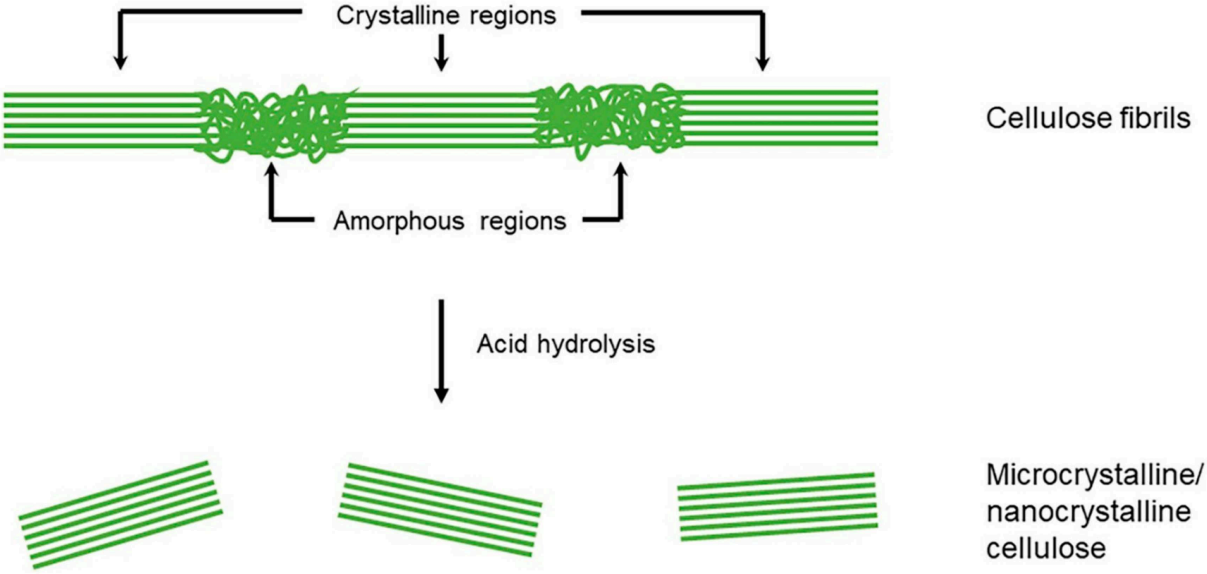

Figure 8. Formation of MCC/CNC by acid hydrolysis [16].

Hosseinpour et al. [64] investigated the improvement in DMFC performance using multilayer membranes with the addition of nanocrystalline cellulose (CNC). Methanol permeability through fuel cell membranes significantly reduces DMFC efficiency, aiming at decreasing methanol permeability while maintaining high proton conductivity. CNC was used as an economical and biodegradable barrier material within a multilayer membrane of the same thickness as a standard Nafion N115 membrane. Nanocrystalline cellulose, with fibre widths of 5–20 nm and lengths of 140–200 nm, was added as a barrier layer by spraying onto the multilayer membrane structure. The optimal CNC content was 1.5 wt%. By placing a CNC film between the layers of NR211 and NR212 Nafion membranes, closer to the anode, the methanol crossover was effectively blocked. The CNC-doped membrane (ML-CNC-2), prepared by pressing at room temperature, showed an 11% reduction in methanol permeability compared to Nafion N115. This resulted in a 38% improvement in DMFC performance over standard Nafion N115.

The fabrication of composite biopolymer membranes using microcrystalline cellulose (MCC) modified with phosphotungstic acid (PTA) and imidazole was discussed by Bagus Pambudi et al. [65]. The modified membranes exhibited higher proton conductivity: the membrane with imidazole (Cell-Im) showed three times higher conductivity, while the membrane with phosphotungstic acid (Cell-PTA) demonstrated 1.5 times higher conductivity compared to the pure cellulose membrane. Both composite membranes also displayed lower methanol permeability, making them suitable candidates for DMFCs.

Muhmed et al. [66] investigated the effect of CNC on membrane properties for DMFCs. CNC was synthesised by hydrolysing MCC with sulphuric acid at different concentrations (30%, 40%, 50%), and then mixed with poly (vinylidene fluoride), PVDF, to obtain

composite membranes. The results showed that the CNC-3/PVDF membrane, prepared with 50% sulphuric acid, had a low swelling rate (15.19%) and low methanol permeability (2.69×10^{-9} cm^2/s) compared to Nafion 117. The high crystallinity of CNC and the hydrophobicity of PVDF contributed to improved dimensional stability and reduced methanol permeability. Although the proton conductivity of the CNC-3/PVDF membrane was lower (0.0757 mS/cm), its selectivity (28.14×10^3 Ss/cm^3) was significantly higher than that of Nafion 117 due to improved barrier properties.

The influence of adding microcrystalline cellulose and 2,3-dialdehyde cellulose (DAC) on the properties of highly sulfonated poly (ether ether ketone) (SPEEK) for use in DMFCs was investigated by Ben Moussa et al. [67]. MCC and DAC were incorporated into the SPEEK matrix at different ratios (3%, 6%, 9%) to improve the proton conductivity and mechanical properties of the membranes. Proton conductivity tests at 100% relative humidity (RH) in water showed that the optimal MCC content is 3 wt%, while the optimal DAC content is 6 wt%. However, when tested at 100% RH in methanol, the optimal MCC content is 6 wt%, and the optimal DAC content is 3 wt%. SPEEK/MCC-3 achieved the highest proton conductivity of 186 mS/cm at 110 °C, while SPEEK/DAC-6 reached 152 mS/cm at 110 °C. The enhancement in proton conductivity was ascribed to hydrogen-bond interactions between cellulose hydroxyl groups and the sulfonic acid groups of SPEEK, which promote more efficient proton transport. Additionally, the incorporation of MCC and DAC reduced methanol uptake, which is crucial for reducing fuel permeability in DMFC applications.

The influence of different acids (citric, phosphoric, and their mixtures) on cellulosic filter papers for use in PEMFCs was investigated by Raut et al. [68]. Treating cellulose with acids enabled hydrolysis and the formation of additional proton-conducting pathways, increasing the ion exchange capacity (IEC) to 0.1 meq/g for cellulose filter papers treated with a mixture of acids. Furthermore, impregnation with resorcinol bis(diphenyl phosphate) (RDP) reduced gas permeability and improved proton conductivity. The membrane treated with a mixture of acids and RDP achieved the highest output power of 16.1 mW/cm^2 with air and 34.3 mW/cm^2 with oxygen, maintaining stable operation for 100 h. A more detailed analysis confirmed that acids alter the way RDP binds to cellulose, thereby increasing proton mobility. These results are summarised in the polarisation curves shown in Figure 9, which illustrate the performance of the various cellulose/RDP membranes under different conditions. This study demonstrates that simple modifications to cellulosic filter papers can produce efficient and sustainable membranes for lower-power PEMFC applications.

2.2.2. Cellulose Nanofibres

Cellulose nanofibres (CNFs) are commonly obtained by mechanically processing plant-derived biomass that has been pretreated with sodium hypochlorite and sodium hydroxide to remove lignin and hemicellulose. In top-down fabrication methods, including high-pressure homogenisation, microfluidisation, refining, and grinding, applied shear forces break down cellulose microfibres into nanoscale fibrils. This process produces fibres with diameters usually between 10 and 200 nm and lengths of several micrometres [69]. As an alternative, CNFs may be produced through a bottom-up route involving the hydrolysis of electrospun cellulose acetate, a method that enables the formation of fibres with greater lengths compared to mechanically derived CNFs. [70]. Due to the inherent mechanical strength of cellulose and the abundance hydroxyl functional groups, CNFs are suitable for chemical modification and form interconnected networks, enabling their use as reinforcing support matrices in composite materials. The production pathways for CNFs, including both top-down and bottom-up approaches, are shown in Figure 10.

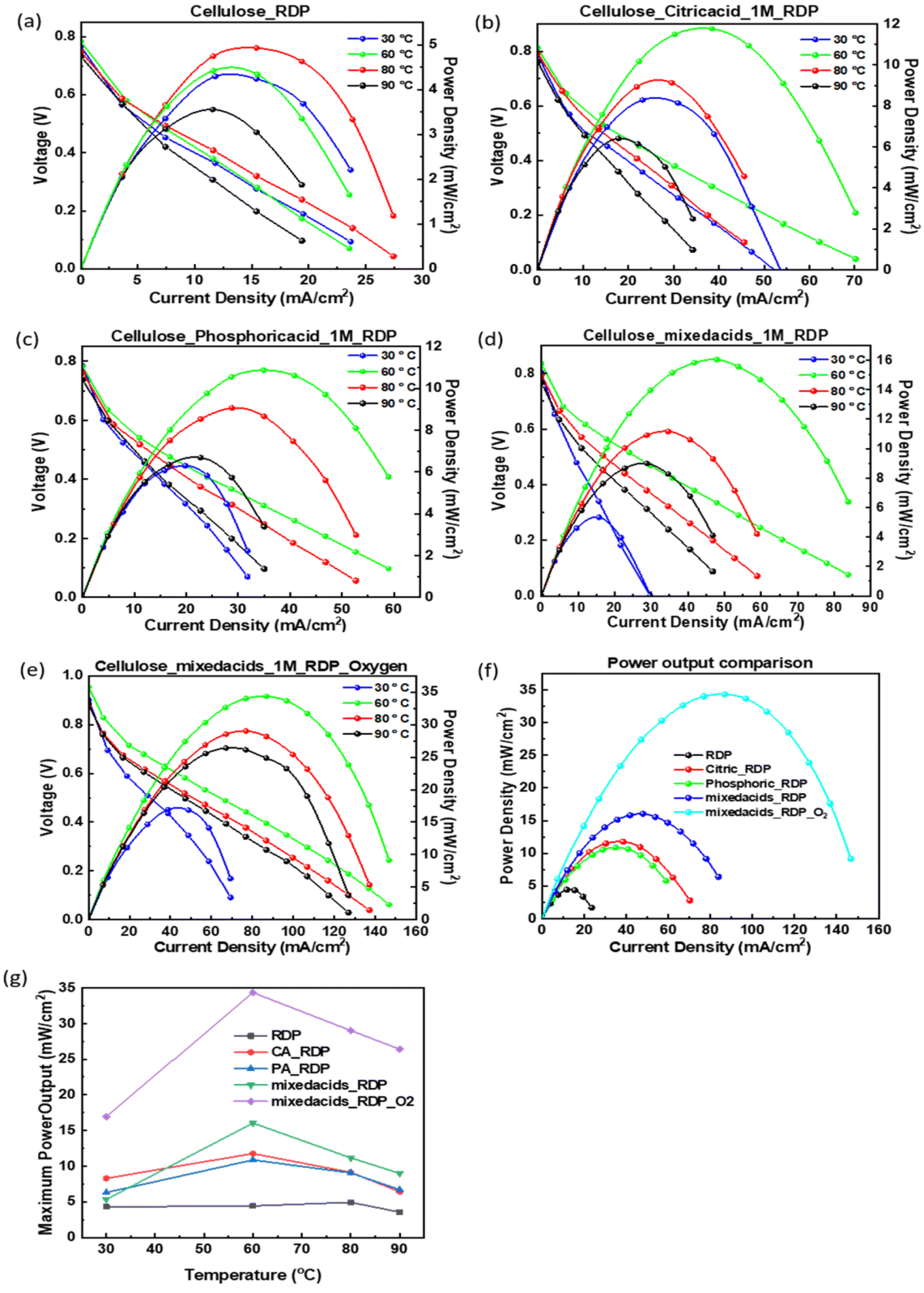

Figure 9. Polarisation curves for cellulose/RDP membrane with (**a**) untreated, (**b**) citric acid, (**c**) phosphoric acid, (**d**) mixed acids, and (**e**) mixed acids in oxygen environment; (**f**) comparison of maximum power performance for the respective membrane–electrode assembly (MEA); (**g**) comparison of power performance as a function of temperature for each MEA [68].

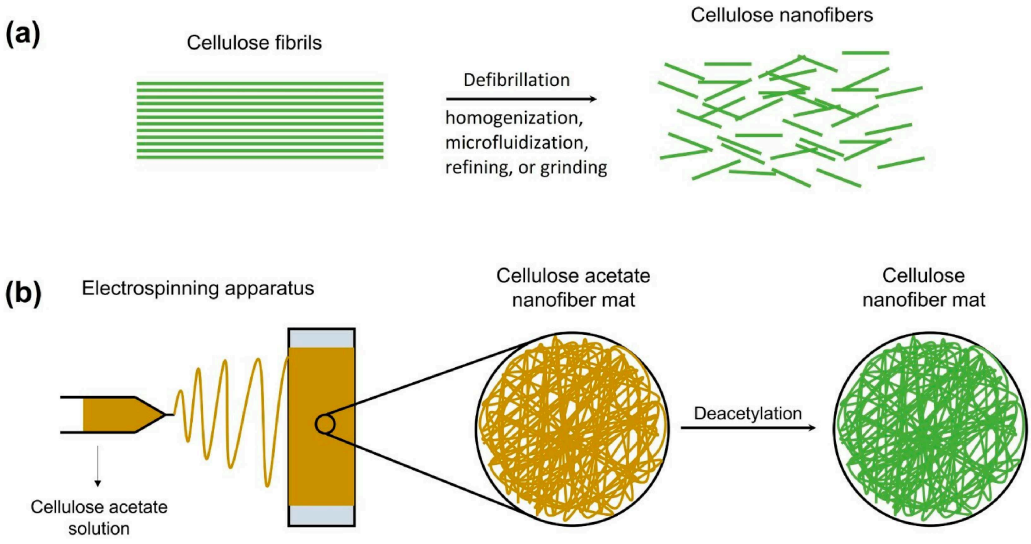

Figure 10. Creating CNFs via (**a**) top-down methods, such as grinding, and (**b**) bottom-up methods, such as electrospinning and hydrolysis [16].

Bayer et al. [71] investigated biopolymer membranes based on sulfonated cellulose nanofibres (S-CNF) as an alternative to expensive fluoropolymer membranes such as Nafion. Three types of membranes were used: common nanocellulose (CNF), crystalline nanocellulose (CNC), and sulfonated nanocellulose (S-CNF). CNF showed excellent mechanical strength but low proton conductivity, while CNC had higher conductivity but poor mechanical stability. S-CNF membranes exhibited a proton conductivity of 2 mS/cm and a significantly lower hydrogen permeability than Nafion, demonstrating potential for fuel cell applications. One membrane was produced by a spraying process, in which a sulfonated nanocellulose suspension was uniformly applied directly to the electrocatalytic layer, in a process similar to 3D printing. Thin membranes (8 µm) produced by this method enabled a high current density (>0.8 A/cm^2) and a power density of 156 mW/cm^2. The main challenges were low open-circuit voltage due to occasional microcracks in the membrane and the need for process optimisation. Figure 11 presents the polarisation and power density curves for these S-CNF membranes, along with comparisons of hydrogen permeability and durability tests. However, its extremely low cost ($50/m^2) and biodegradability make this technology promising for commercial and disposable applications.

An investigation of biopolymer membranes made from cellulose nanofibres (CNFs) derived from wood pulp was conducted by Li et al. [72]. Four types of membranes were used: CNF-1 (without cross-linking with citric acid), CNF-2 and CNF-4 (with low and high proportions of citric acid), and CNF-3 (with optimal cross-linking using 0.300 mL 1 M citric acid). CNF-3 showed the best performance with a conductivity of 9.4 mS/cm and a power density of 27.7 mW/cm^2 at 80 °C, which was 30 times higher than that of the non-cross-linked membrane (CNF-1). The manufacturing process involved TEMPO oxidation of the wood pulp, cross-linking with citric acid, and drying and thermal pressing. Cross-linking with citric acid increased mechanical flexibility, reduced porosity, and improved proton conductivity due to the formation of ester bonds and additional carboxyl groups, as illustrated in Figure 12, showing polarisation curves and power density curves for all membranes.

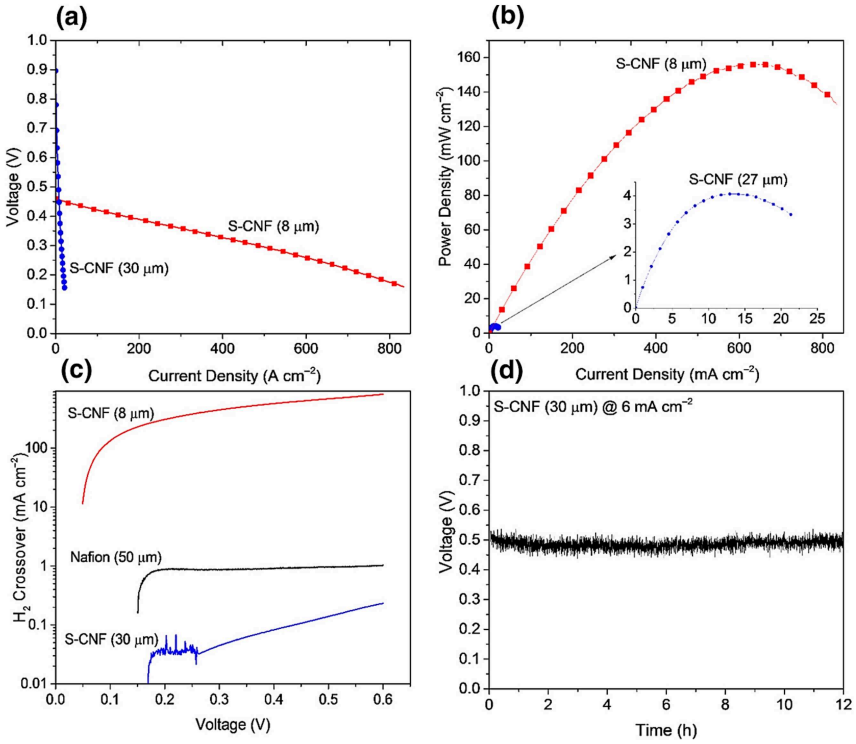

Figure 11. Polarisation curves and power density curves of membrane fuel cells: (**a**) S-CNF with a thickness of 30 µm and (**b**) S-CNF with a thickness of 8 µm; (**c**) comparison of hydrogen permeability current density for Nafion and biopolymer membranes based on S-CNF; (**d**) durability test of a fuel cell with a S-CNF membrane with a thickness of 30 µm [71].

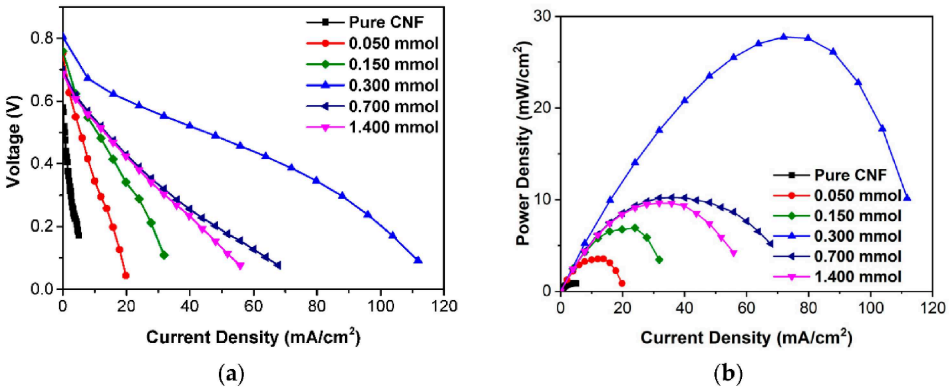

Figure 12. (**a**) Polarisation curves and (**b**) power density curves of all membranes [72].

2.2.3. Bacterial Cellulose

Bacterial cellulose (BC) is a highly crystalline extracellular substance produced by various bacterial species. High-yielding species such as *Gluconacetobacter xylinus* (also known as *Acetobacter xylinum* and *Komagataeibacter xylinus*) show promising potential for industrial production [73]. BC forms a three-dimensional nanofibrous network with fibre diameters approximately two orders of magnitude smaller than those of plant-derived cellulose, contributing to its superior tensile strength, higher crystallinity index, and enhanced water-holding capacity [74]. In addition to these structural advantages, BC is exceptionally pure, being inherently free from lignin and hemicellulose. The abundance of reactive hydroxyl groups within its cellulose framework enables diverse chemical functionalisation strategies, including the introduction of groups that promote ionic conductivity.

Yang et al. [75] investigated two types of biopolymer membranes based on bacterial cellulose: an unmodified membrane (Unmodified-BC) and a membrane modified with

3-aminopropyltriethoxysilane (APTES) (Modified-BC). The unmodified membrane showed very poor water stability and low proton conductivity, whereas the modified membrane demonstrated significantly improved properties. The highest proton conductivity of the modified-BC membrane was 62.2 mS/cm at 95 °C and 100% RH, and the maximum power density in the fuel cell was 4.85 mW/cm^2. The open-circuit voltage of the fuel cell was 0.92 V, and the membrane maintained stable operation for one hour under constant load. The membrane was prepared by solution casting after APTES was hydrolysed and chemically bound to the surface of the bacterial cellulose. Despite its lower conductivity compared to Nafion, the advantages of this membrane include high mechanical strength (86 MPa), chemical stability, and a cost ten times lower, making it suitable for biodegradable and disposable hydrogen fuel cells, as shown in Figure 13.

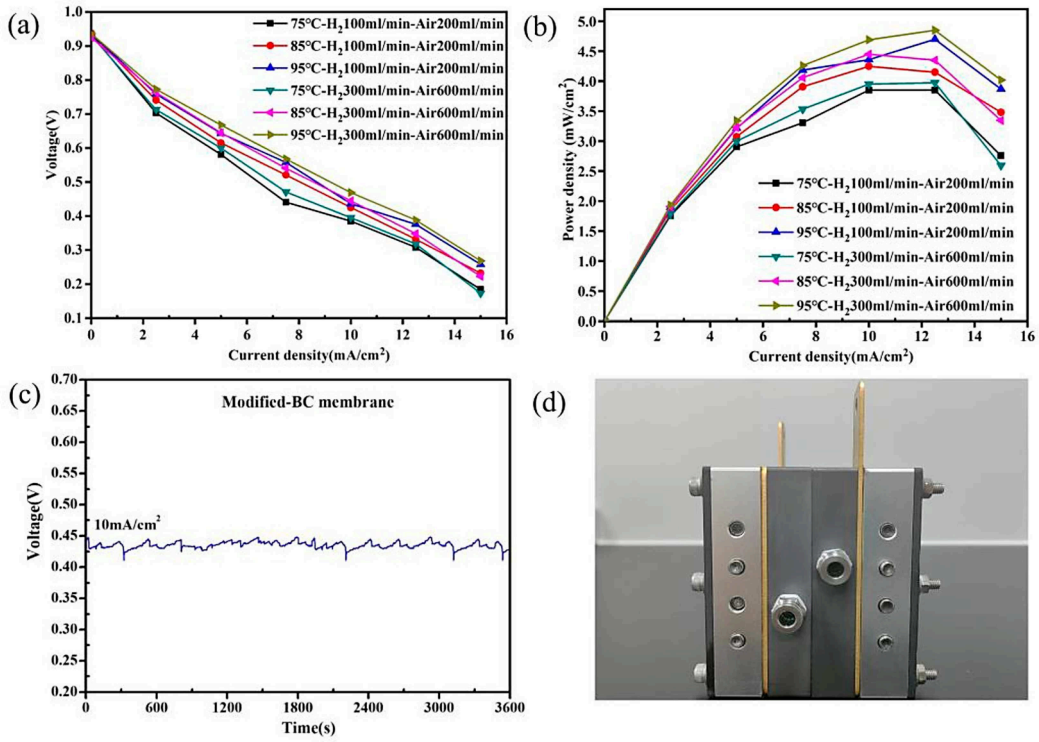

Figure 13. (**a**) Polarisation curves of a single fuel cell at 100% RH, (**b**) power density curves at 100% RH, (**c**) output voltage stability at 100% RH and 85 °C for a current density of 10 mA/cm^2, and (**d**) photograph of a single fuel cell used for tests [75].

2.2.4. Cellulose Acetate

Cellulose acetate (CA) is a chemically modified form of cellulose in which up to three hydroxyl groups per anhydroglucose unit are substituted with acetyl groups. The classification of CA depends on its degree of substitution (DS), and it is categorised as monoacetate (DS < 2.2), diacetate (DS = 2.2–2.7), or triacetate (DS = 2.7–3.0) [76]. This substitution process interferes with natural crystallinity, increasing cellulose solubility in widely used organic solvents. For example, cellulose diacetate is soluble in acetone, unlike raw cellulose, making it suitable for reshaping techniques such as spinning. As the acetyl group content increases, the inherent hydrophilicity of the cellulose structure decreases [77].

Khalifa et al. [78] developed biopolymer membranes based on phosphorylated cellulose acetate matrix (Ph-CA) with the addition of titanium dioxide nanoparticles (TiO_2) in various proportions (0, 2.5, 5, 7.5, and 10 wt%). The membranes were designated as TiO_2/Ph-CA-x, where "x" represents the weight percentage of TiO_2. The best performance was observed with 5 wt% TiO_2, where the membrane showed the highest IEC (1.13 meq/g at 25 °C and 2.01 meq/g at 80 °C) and the lowest methanol permeability

(0.98×10^{-16} cm^2/s), which is significantly better than Nafion (1.14×10^{-9} cm^2/s). The mechanical strength of the membrane with 7.5 wt% TiO_2 was 58 MPa, while the contact angle indicated good hydrophilicity up to 5 wt%. The addition of more than 5 wt% TiO_2 resulted in decreased IEC and hydrophilicity due to particle agglomeration. The membranes demonstrated good thermal stability and chemical resistance to Fenton's solution. Figure 14 shows how the performance factor changes with TiO_2 content, indicating an optimal 5 wt% content. In conclusion, the optimal proportion of TiO_2 was 5 wt%, at which the best overall performance was achieved for application in DMFCs.

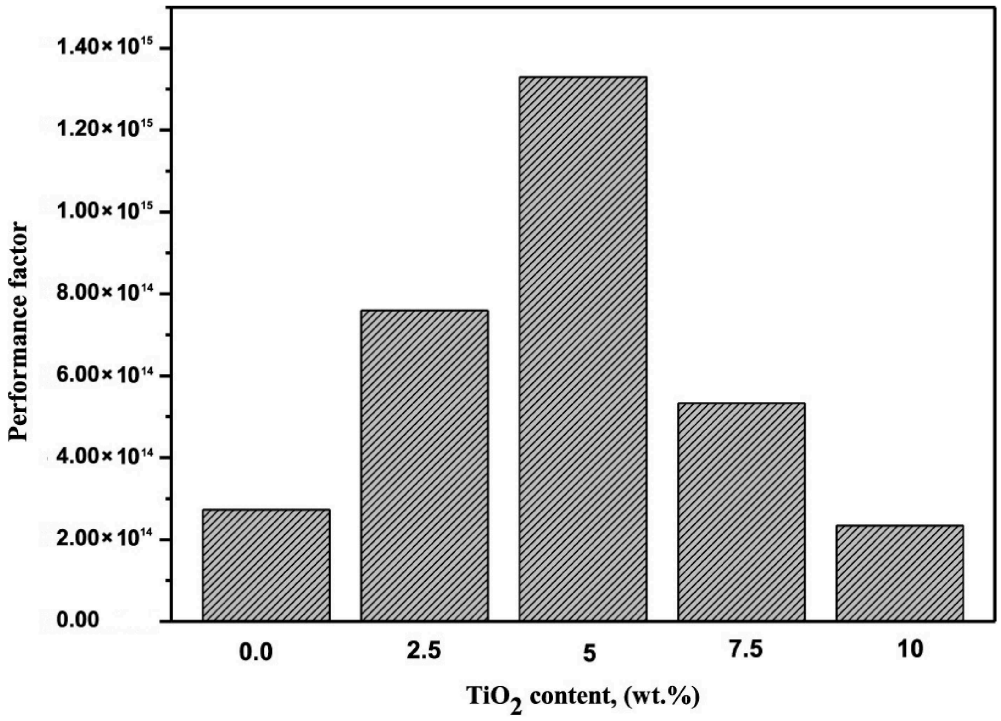

Figure 14. Performance factor as a function of TiO_2 nanoparticle content [78].

Biopolymer membranes based on cellulose acetate (CA) reinforced with graphene oxide (GO) nanoparticles in various proportions (from 0.05 to 0.8 wt%) were developed by Madih et al. [79]. Seven types of membranes were tested, designated as CA-GO-X, where X indicates the weight percentage of GO. The membrane with the highest GO content (0.8 wt%) showed the best properties: a proton conductivity of 15.5 mS/cm and a power density of 519 mW/cm^2 at 60 °C and 100% RH, both higher than those of Nafion 212 (401 mW/cm^2). Increasing the GO proportion improved IEC (up to 1.18 meq/g), water absorption (up to 24%), and mechanical strength (up to 58 MPa), but reduced thermal stability. The pure CA membrane had significantly lower conductivity (1.21 mS/cm) and power density (235 mW/cm^2), whereas the composite membranes showed gradual improvements with increasing GO content, as shown in the polarisation and power density curves for all membranes (Figure 15). Membranes containing 0.3–0.5 wt% GO also achieved competitive performance with balanced mechanical and electrochemical properties. These results are particularly significant because the membranes were fabricated by simple solution casting, indicating their potential for the environmentally friendly and low-cost production of PEM fuel cells.

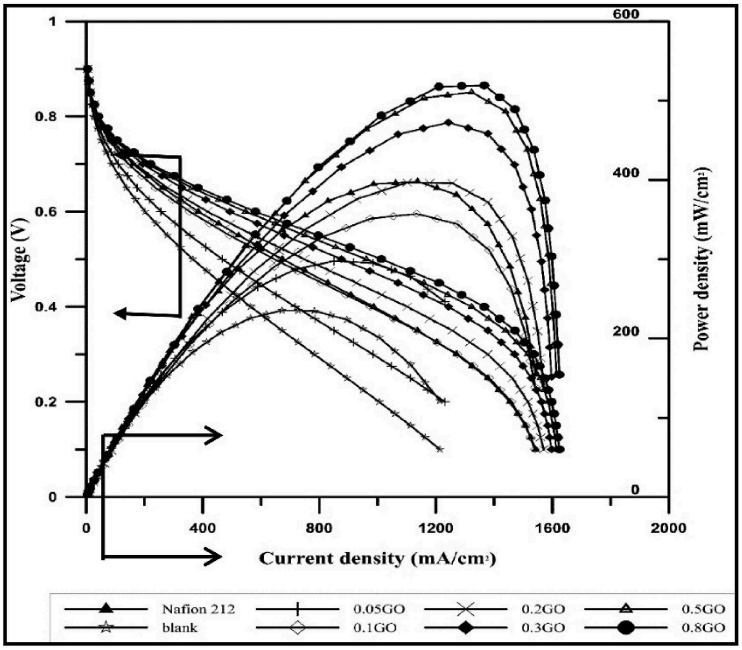

Figure 15. Polarisation curves and power density curves for pure CA membrane, CA/GO nanocomposite membranes and Nafion 212 [79].

Khalaf et al. [80] prepared phosphorylated PEMs based on polyvinyl alcohol (PVA) and cellulose acetate (CA) for use in DMFCs. The membranes were synthesised using the solution casting technique, and their properties were examined as a function of CA content, ortho-phosphoric acid (OPA) concentration, and glutaraldehyde (GA) concentration. The results showed that the phosphorylated PVA/CA membranes exhibited proton conductivities of 35 mS/cm at 25 °C and 50 mS/cm at 70 °C, with an ion exchange capacity (IEC) of 2.1 meq/g. In addition, the membranes showed low methanol permeability (1.08×10^{-10} cm^2/s), which is significantly lower than that of Nafion 117 membranes. Phosphorylation improved proton conductivity and mechanical properties, while the addition of CA reduced swelling and improved stability.

2.3. Gellan Gum

Gellan gum, an anionic polysaccharide that dissolves in water, is synthesised by the bacterium *Sphingomonas elode* [81]. This biopolymer can be used alone or blended with secondary components to tailor specific material properties. Notably, it enables the fabrication of thermoreversible membranes that exhibit consistent reversible transitions during thermal cycling. Structurally, gellan gum is classified as a heteropolysaccharide. Its structure is defined by complex tetrasaccharide repeating sequences, which maintain a stoichiometric ratio of 1:2:1 for α-L-rhamnose, β-D-glucose, and β-D-glucuronic acid. Figure 16 shows the structure of gellan gum. It contains a significant number of -OH groups, to which the cation of any salt can be attached to increase the charge carrier concentration. It is available as low acyl, which forms hard, brittle gels, and high acyl, which forms soft, elastic, unbreakable gels. A unique property of gellan gum is its ability to produce a low-viscosity solution. It also has high thermal stability up to 120 °C, which is why it can be used in electrochemical devices [82].

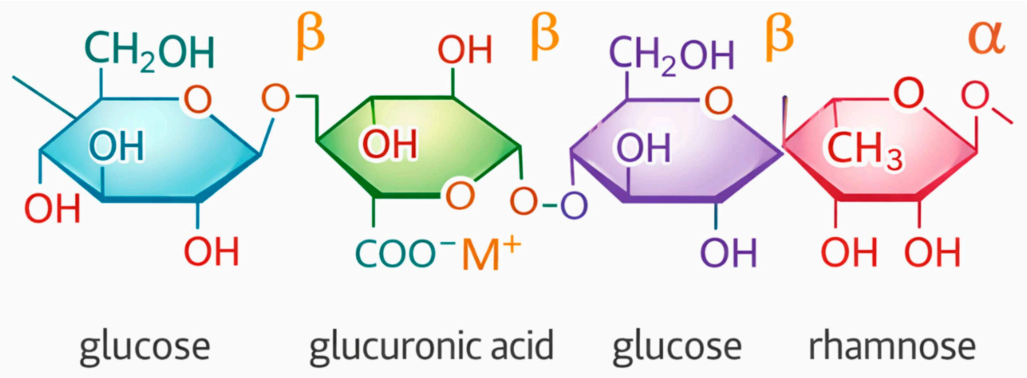

Figure 16. Structure of gellan gum.

Naachiyar et al. [83] developed biopolymer membranes based on gellan gum doped with various concentrations of ammonium thiocyanate (NH_4SCN), ranging from 0.8 to 1.2 wt%. All membranes were prepared by the solution casting method, with the membrane containing 1.1 wt% NH_4SCN exhibiting optimal electrochemical properties. This membrane showed the highest proton conductivity (14.1 mS/cm), the lowest crystallinity (8.85%), and a low glass transition temperature (42.98 °C), indicating a high degree of amorphousness suitable for proton transport. The best-performing membrane was used to construct a single PEM fuel cell, which achieved an output voltage of 0.58 V. The same membrane was also used to fabricate a proton battery with an open-circuit voltage of 1.62 V and a discharge duration of 60 h at low load. These results demonstrate the significant potential of gellan gum as a sustainable and efficient material for electrochemical devices.

2.4. Sodium Alginate

Extracted from brown seaweed of the *Laminariaceae* family, sodium alginate (SA) is a hydrophilic anionic polysaccharide. Its main industrial sources are the species *Laminaria hyperborea*, *Macrocystis pyrifera*, and *Ascophyllum nodosum* [84]. Structurally, SA is a branched polymer composed of β-(1→4)-linked D-mannuronic acid and α-(1→4)-linked L-guluronic acid residues. Because of its biodegradability, biocompatibility, and low toxicity, SA is an effective stabilising and gelling agent. As a result, it is widely used in pharmaceuticals, food processing, and cosmetics. However, the use of pristine SA membranes is often limited by certain drawbacks, particularly their tendency to swell significantly and their suboptimal mechanical stability [85].

Shaari et al. [86] prepared biopolymer membranes based on sodium alginate, incorporating varying amounts of titanium dioxide (TiO_2) nanoparticles, labelled as SAT1 to SAT5, containing 5–25 wt% TiO_2. All membranes were tested in a single DMFC, with the SAT4 membrane containing 20 wt% TiO_2, demonstrating the best performance. This membrane had the highest proton conductivity of 16.8 mS/cm at 30 °C, the lowest methanol permeability (1.95×10^{-7} cm^2/s), and the highest selectivity of 8.615×10^4 Ss/cm^3. In the single PEM fuel cell, the SAT4 membrane achieved a maximum power density of 19.13 mW/cm^2 at 60 °C, which is higher than that of Nafion 117 (13.63 mW/cm^2) under the same conditions. The mechanical strength was 4.3 MPa, and the membrane also showed good chemical resistance, remaining intact after 192 h in 2 M methanol at 60 °C. Compared with other biopolymer membranes based on SA (e.g., SA/glycerine, SA/SGO), SAT4 provides the best balance of conductivity, stability, and selectivity. The performance differences are further illustrated in Figure 17, showing polarisation and power density curves for Nafion 117 and SAT4 in a methanol concentration of 4 M at 30 °C and 60 °C.

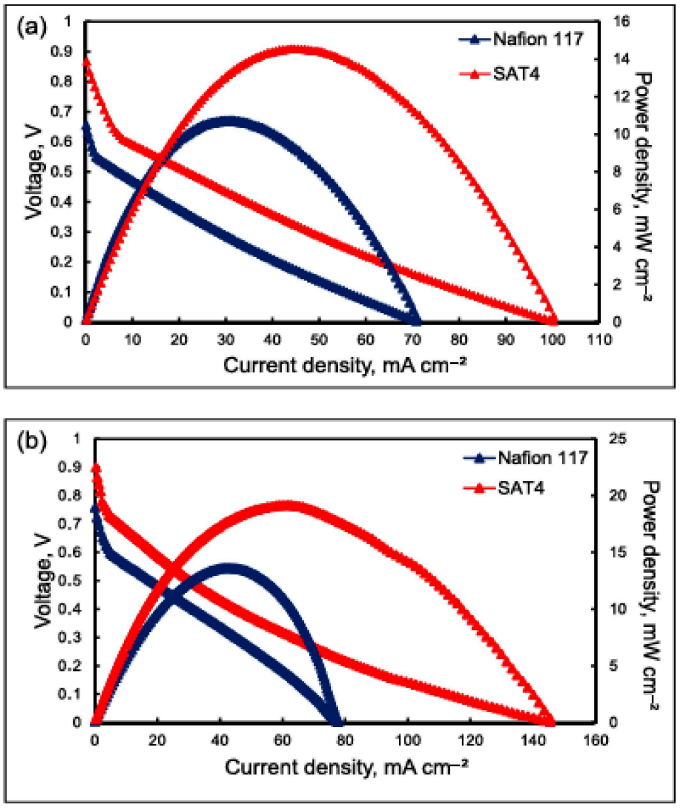

Figure 17. Polarisation curves and power density curves obtained for Nafion 117 and composite membrane SAT4 with 4M methanol concentration at temperature of 30 °C (**a**) and 60 °C (**b**) (reprinted with permission from ref. [86]. Copyright (2019) Wiley Online Library).

Vijitha et al. [87] prepared four types of biopolymer membranes based on sodium alginate, which were sulfonated using two monomers, namely 2-acrylamido-2-methyl-1-propanesulfonic acid (SA-g-AMPS) and sodium 4-vinylbenzenesulfonate (SA-g-SVBS), then blended with polyvinyl alcohol (PVA). The resulting membranes were designated PSAAM and PSASB, while their composite versions, incorporating 10 wt% phosphomolybdic acid (PMA), were named PSAAM-PMA and PSASB-PMA. The PSAAM-PMA membrane showed the highest proton conductivity of 59.23 mS/cm, while PSASB-PMA reached 45.66 mS/cm. Both composite membranes also demonstrated low methanol permeability (1.36×10^{-6} cm^2/s and 1.61×10^{-6} cm^2/s), significantly better than the pure membranes. Various characterisation techniques confirmed good homogeneity and stability.

Yusoff et al. [88] investigated sodium alginate (SA)-based biopolymer membranes cross-linked with glutaraldehyde (GA) and plasticised with 5 wt% glycerol to improve their ionic and mechanical properties for fuel cell applications. Five different membranes (SA-5 to SA-25) containing 5–25 wt% GA were prepared. The highest proton conductivity was achieved by the SA-15 membrane with a value of 8.28 mS/cm, while the highest ion exchange capacity (IEC) was observed in SA-25 (1.293 meq/g). In terms of mechanical properties, the SA-25 membrane had the highest tensile strength (251.39 MPa), while the SA-15 and SA-20 membranes also demonstrated good strength with reduced elasticity. These trends in swelling ratio, water uptake, and methanol uptake of the cross-linked SA membranes are summarised in Figure 18.

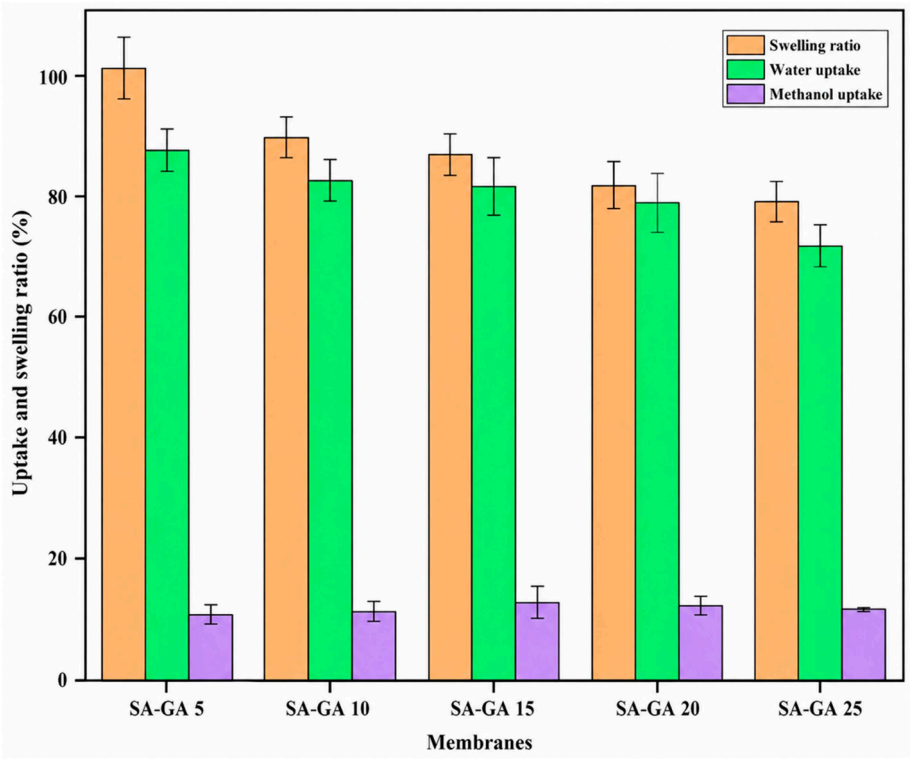

Figure 18. Swelling ratio, water uptake and methanol uptake of cross-linked SA membranes [88].

2.5. Starch

Starch, a plant-derived natural polysaccharide, has become a focal point of research into sustainable and biodegradable materials. It shows significant promise for energy storage technologies and electrolyte systems [89]. Due to its cost-effectiveness and ability to produce flexible films, it is considered as a suitable substrate for proton exchange membranes (PEMs) [90]. The performance of starch-based membranes can be improved by incorporating salts, such as sodium hydrogen sulphate (SHS). These composites are expected to demonstrate enhanced ionic conductivity and superior mechanical stability, thereby increasing their suitability for use in fuel cells and related electrochemical applications [91].

Composite membranes based on starch and chitosan for use in hydrogen fuel cells were investigated by Al-Othman et al. [92]. The pure starch membrane achieved a proton conductivity of 2.1 mS/cm but was mechanically fragile. Adding chitosan in ratios of 23–48 wt% improved both proton conductivity and mechanical properties, with the optimal ratio of 38 wt% chitosan resulting in a conductivity of 2.8 mS/cm. The influence of the ionic liquid diethylmethylammonium methanesulfonate on the membrane properties was also examined. However, the addition of the ionic liquid reduced proton conductivity by 45–65%, indicating a negative impact on performance.

Faiz Hassan et al. [93] investigated biopolymer membranes based on starch and sodium hydrogen sulphate (SHS) prepared by the solution casting method. Pure starch membranes were transparent and mechanically unstable, whereas the addition of SHS at concentrations of 5–45 wt% altered morphology and structure. Figure 19 illustrates how varying SHS content affects the proton conductivity of these starch-based membranes. The membrane with 15 wt% SHS achieved the highest ionic conductivity of 0.0317 mS/cm, attributed to an increase in the number of mobile ions and a decrease in crystallinity. However, a further increase in SHS concentration (up to 45 wt%) led to a decrease in conductivity due to ion aggregation and structural changes. Scanning electron microscope (SEM) analysis showed that the addition of SHS changes surface morphology, from smooth

to rough and uneven, affecting the mechanical properties. Other analyses confirmed interactions between starch and SHS and structural changes.

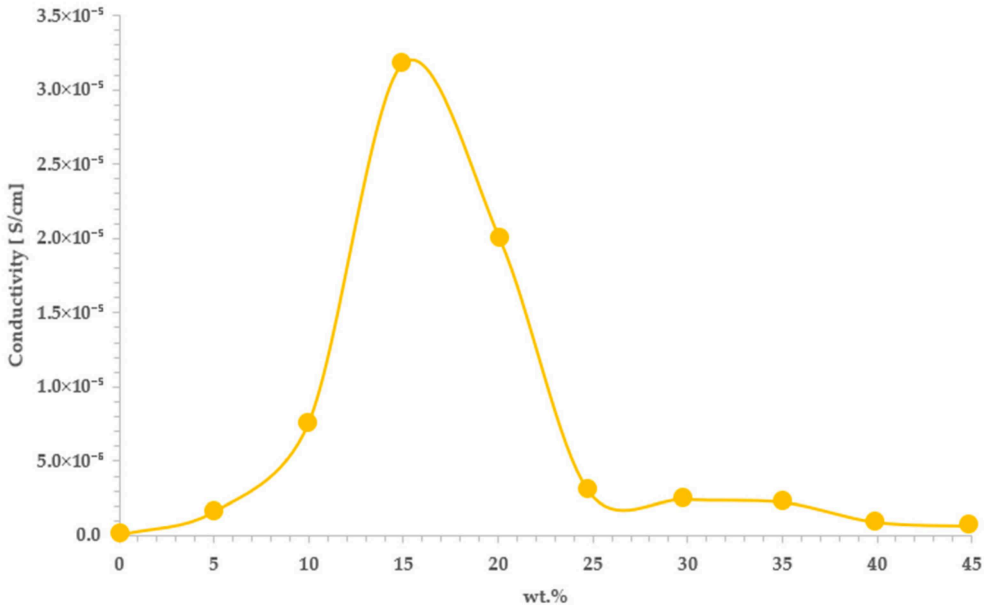

Figure 19. Proton conductivity of starch-based biopolymer membranes with different weight percentages of sodium hydrogen sulphate (SHS). Based on data from [93].

2.6. Keratin

Keratin is a proteinaceous biopolymer notable for its impressive mechanical durability and inherent capacity for self-assembly [94]. These proteins are generally categorised into "hard" varieties, sourced from hair, and "soft" types, originating from epithelial tissues. Hard keratins have a higher concentration of cysteine residues, which enables a more extensive network of sulphur-based cross-linking [95]. Due to their fibrous nature, keratins are exceptionally stable and exhibit low solubility. Keratins are further classified as either α-keratins or β-keratins based on their secondary structure. α-keratins possess a tightly coiled, right-handed helical configuration with 3.6 amino acids per turn. Hydrogen bonding within the side chains stabilises this tertiary arrangement. In general, β-keratins are predominantly found in reptiles and birds. These structures achieve stability through extensive hydrogen bonding between the carboxyl and amino groups. Notably, β-keratins are significantly more difficult to extract than their α counterparts [96]. For energy applications, keratins are highly useful due to the presence of nitrogen atoms that enhance carbon activation for ion transport, as well as biopolymer properties such as biodegradability [97].

Soon et al. [98] investigated keratin membranes derived from industrial chicken feather waste for use in PEM fuel cells. The membranes were prepared by extracting keratin, forming amyloid fibres through heat treatment, and applying oxidative modification to increase proton conductivity. The modified keratin membranes (Keratin-M) achieved an ion exchange capacity of 1.56 meq/g and a proton conductivity of 6.3 mS/cm in water, both significantly higher than those of untreated membranes. Additionally, the membranes showed threefold lower methanol permeability compared to Nafion, making them promising candidates for DMFCs. The performance of a single PEM fuel cell using the keratin membrane, under hydrogen/air and hydrogen/oxygen conditions, is shown in Figure 20. Testing in a single PEM fuel cell demonstrated a maximum power density of 25 mW/cm^2 at 55 °C, and the membranes have also been successfully used in proton transistors and electrolysers for hydrogen production. These results highlight the potential of keratin membranes as a low-cost and sustainable alternative to commercial PEM membranes.

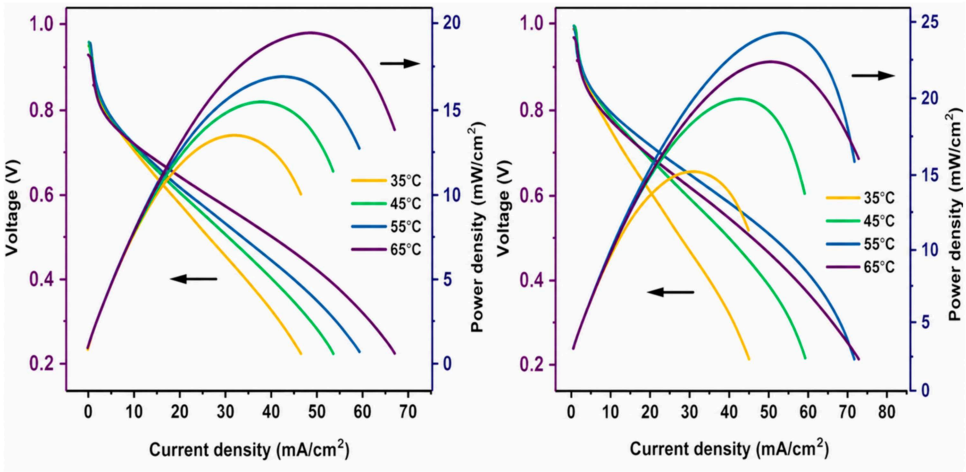

Figure 20. Performance of a keratin membrane single fuel cell with hydrogen and air (**left**), and hydrogen and oxygen (**right**) (reprinted with permission from ref. [98]. Copyright (2023) ACS Publications).

Biopolymer membranes based on bacterial cellulose and keratin from human nails, prepared in different mass ratios (4.5:0.5, 4.3:0.7, and 4:1), were investigated by Gustian et al. [99]. The analysis confirmed interactions between bacterial cellulose and keratin through hydrogen bonds and showed that the membranes have a semicrystalline structure, contributing to their mechanical strength. The highest proton conductivity was achieved with the membrane at a 4:1 ratio (0.04572 mS/cm at 25 °C), while the degree of swelling was 32.50%. These results suggest that adding keratin improves proton conductivity by providing amino groups that facilitate proton transfer. Although the membranes' performance remains lower than that of Nafion, these studies highlight the potential of bacterial cellulose and keratin as low-cost, sustainable alternatives for fuel cell applications. The membranes also showed good thermal stability and mechanical properties, making them promising materials for further development.

2.7. Collagen

As the predominant structural protein in biological systems, collagen is a protein-based biopolymer essential for tissue integrity [100]. It is characterised by a sophisticated, hierarchical fibrous architecture that culminates in a triple-helix quaternary structure known as tropocollagen. These tropocollagen units further assemble to form robust collagen fibres. This intricate polymer arrangement gives collagen with superior mechanical properties, particularly high tensile strength and elasticity [101]. Chemically, collagen contains a high density of carbon, nitrogen, and oxygen atoms. This atomic composition enables doping strategies to enhance the electrochemical performance of biopolymer-based membranes [102]. Notably, for energy applications, collagen is often recovered from leather and skin waste. Using such by-products demonstrates a commitment to the circular economy and the development of sustainable materials for green energy storage [103].

Proton conduction in collagen does not occur through the collagen molecule itself, but mainly through water molecules hydrated around it (Figure 21). The collagen triple-helix structure provides sites (N-H, O-H, and C=O groups) where water molecules attach via hydrogen bonding, forming a hydration shell. At low hydration levels ($N < 2$ water molecules per unit), these water molecules are isolated, so proton transport is negligible. As hydration increases ($2 < N < 4$), water molecules form intra-water bridges inside the helix, enabling limited, quasi-one-dimensional proton transfer. At higher hydration levels ($N > 4$), excess water molecules begin linking adjacent helices via inter-water bridges, and by around $N \approx 7$, these connections evolve into a continuous three-dimensional

hydrogen-bonded network. This extended network allows efficient long-range proton conduction [104,105].

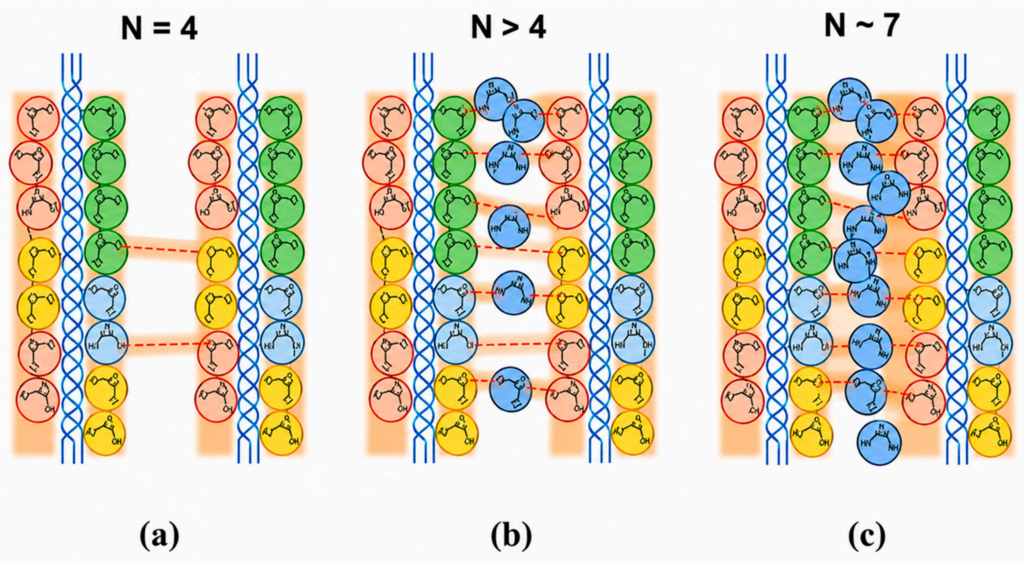

Figure 21. Inter-water bridge formed in between adjacent helices. (**a**) Weak inter-water bridge (red broken lines) because of the large hydrogen-bonding distance at N = 4; (**b**) the bridge strengthened with the increasing water molecules at N > 4; (**c**) proton conduction via the three-dimensional water network established in between the helices [104].

Biopolymer membranes composed of collagen and imidazole were investigated by Furuseki et al. [106] to achieve anhydrous proton conductivity, i.e., conductivity without the need for moisture. Two types of membranes were tested: pure collagen and imidazole–collagen composites, with the imidazole concentration varied from 0 to 4 wt%. Optimal proton conductivity was achieved in the composite with 2 wt% imidazole, yielding a measured conductivity of about 1 mS/cm at 200 °C. This value surpasses that of other biological anhydrous conductors such as hydroxyapatite–collagen membranes. Experimental measurements showed that conductivity increases with the proportion of imidazole up to 2 wt%, after which it decreases due to the inhibition of imidazole rotation, which prevents proton transfer. It was shown that conductivity perpendicular to the direction of collagen fibres is ten times higher than that parallel to them, confirming the model of proton transfer through breaking and re-establishing hydrogen bonds between imidazole and collagen side chains. This anhydroconductive biomembrane shows potential for application in PEM fuel cells at high temperatures without the need for additional humidification.

Ali et al. [107] developed four types of biopolymer membranes composed of collagen, chitosan, and ionic liquid, with varying amounts of poly(ethylene glycol) (PEG) as a plasticiser. All membranes were prepared by the solution casting method, aiming to improve proton conductivity and elasticity for use in PEM fuel cells. The first membrane, without PEG had the lowest conductivity of 0.062 mS/cm, while the fourth membrane, with the highest PEG content (0.5 g), achieved the highest conductivity of 1.173 mS/cm. The addition of PEG improved conductivity by promoting the dissociation of ion pairs, and all membranes showed high elasticity. However, the conductivity remains lower than that of Nafion (100 mS/cm), so further optimisation of the composition, particularly the amounts of ionic liquid and chitosan, was suggested. The authors also proposed testing hydrated membranes and assessing their stability at elevated temperatures to improve their applicability in high-temperature PEM systems.

Several affordable proteins, which are primarily produced from waste sources of the food industry, could also make proton-conducting biopolymers. This group of proteins

contain: (1) The milk-derived casein protein that can form proton-conducting films upon its chemical sulfonation with proton conductivity values of 0.4 mS/cm [108]. (2) The glyco-sylated mucin protein that can form proton-conducting films upon its chemical carboxyla-tion with proton conductivity values of 2.1 mS/cm [109]. (3) The bovine serum albumin (BSA) protein that can be electrospun to mats with proton conductivity in the order of 0.5-1 mS/cm [110,111]. The BSA mats can be further doped with carbon dots, which showed an increase in proton conductivity to 3.5 mS/cm [112]. The BSA protein can also form films, which showed even increased proton conductivity of 5.3 mS/cm [113]. Due to their low cost and sustainability, these protein groups are good biopolymeric candidates for PEM applications.

2.8. Summary of Biopolymer Membrane Properties

Tables 1–3 summarise the main properties of the biopolymer membranes discussed in this study, including proton conductivity, methanol permeability, membrane selectivity, and the maximum power density achieved in a single PEM fuel cell.

Table 1. List of proton conductivities of various biopolymer membranes.

Membrane Name	Proton Conductivity [mS/cm]	Experimental Conditions	Ref.
s-CS/PEO/s-GO (6 wt%)	111.11 48.3	80 °C, 100% RH 30 °C, 100% RH	[32]
CH5	19.4 12.1	65 °C, 100% RH RT, 100% RH	[33]
CS/PGO (2.0)	36	/	[39]
PCS/N-CNT-5	45	80 °C, 100% RH	[40]
Chitosan/Fly Ash 10 wt%	6.863	/	[42]
CS-PAni/SiO_2-3	8.39	80 °C, 100% RH	[43]
CS-WQAT-4	35.3	80 °C, 100% RH	[48]
CS-HPA-PTA	12	70 °C, 100% RH	[49]
CS-STA	4.88	25 °C, 100% RH	[50]
M-10	12.4	25 °C, 100% RH	[53]
CS/SO_3H-UiO-66@HNTs-10	46.2 14.9	80 °C, 100% RH 20 °C, 100% RH	[57]
CS/PS@CNT-5	26	RT, 100% RH	[59]
CS/PD@CNT-5	25	RT, 100% RH	[59]
CPCN@IL-3	2.152 1.394	70 °C, 100% RH 30 °C, 100% RH	[60]
ML-CNC-2	62.71	70 °C, 100% RH	[64]
Cell-Im	0.214	RT	[65]
CNC-3/PVDF	0.0757	25 °C, 100% RH	[66]
SPEEK-MCC-3	186	110 °C, 100% RH	[67]
SPEEK-DAC-3	152	110 °C, 100% RH	[67]
Cellulose_mixedacids_1M_RDP	11 4	90 °C, 100% RH 30 °C, 100% RH	[68]
S-CNF	2	120 °C, 100% RH	[71]
CNF-3	9.4	80 °C, 100% RH	[72]

Table 1. *Cont.*

Membrane Name	Proton Conductivity [mS/cm]	Experimental Conditions	Ref.
Modified-BC	62.2	95 °C, 100% RH	[75]
CA-GO-0.8	15.5	RT, 80–85% RH	[79]
MK 14	50 35	70 °C, 100% RH 25 °C, 100% RH	[80]
1 g Gellan gum + 1 M wt% NH_4SCN	14.1	/	[83]
SAT4	70 16.8	30 °C, 100% RH 70 °C, 100% RH	[86]
PSAAM-PMA	59.23	30 °C, 100% RH	[87]
PSASB-PMA	45.66	30 °C, 100% RH	[87]
SA-15	8.28	RT, 100% RH	[88]
Starch/Chitosan 38 wt%	2.8	/	[92]
Starch/SHS 15 wt%	0.0317	/	[93]
Keratin-M	6.3	/	[98]
Composite 4:1	0.04572	25 °C, 100% RH	[99]
Imidazole–Collagen (n = 2.0)	1	200 °C	[106]
0.1 g collagen:0.1 g chitosan + 0.2 g IL + 0.5 g PEG	1.173	/	[107]
Casein	0.4	RT	[108]
Mucin-COOH	2.1	RT	[109]
BSA mats	0.5-1	RT	[110,111]
BSA mats/CDs	3.5	RT	[112]
BSA films	5.3	25 °C, 75% RH	[113]

RT—room temperature; RH—relative humidity.

Table 2. List of methanol permeability and membrane selectivity parameters of various biopolymer membranes.

Membrane Name	Methanol Permeability [cm^2/s]	Selectivity Parameter [Ss/cm^3]	Experimental Conditions	Ref.
CH5	9.3×10^{-1}	2.1×10^{4}	65 °C, 100% RH 2M CH_3OH	[33]
	4.5×10^{-7}	2.7×10^{4}	RT, 100% RH 2M CH_3OH	
Chitosan/Fly Ash 10 wt%	6.3×10^{-6}	1.1×10^{3}	/ 1M CH_3OH	[42]
M-10	5×10^{-8}	2.47×10^{5}	25 °C, 100% RH 2M CH_3OH	[53]
CS/SO_3H-UiO-66@HNTs-10	5×10^{-7}	2.92×10^{4}	20 °C, 100% RH 2M CH_3OH	[57]
	3.2×10^{-6}	1.18×10^{4}	70 °C, 100% RH 2M CH_3OH	
CPCN@IL-3	7.26×10^{-8}	1.92×10^{4}	RT, 100% RH 2M CH_3OH	[60]
ML-CNC-2	4.5×10^{-6}	1.4×10^{4}	70 °C, 100% RH 2M CH_3OH	[64]

Table 2. *Cont.*

Membrane Name	Methanol Permeability [cm^2/s]	Selectivity Parameter [Ss/cm^3]	Experimental Conditions	Ref.
Cell-Im	4.42×10^{-7}	4.838×10^{2}	70 °C, 100% RH 2M CH_3OH	[65]
CNC-3/PVDF	2.69×10^{-9}	28.141×10^{3}	25 °C, 100% RH 1M CH_3OH	[66]
TiO2/Ph-CA-5	0.98×10^{-16}	/	25 °C, 100% RH 2M CH_3OH	[78]
Ph-PVA/CA	1.08×10^{-10}	/	25 °C, 100% RH 2M CH_3OH	[80]
SAT4	0.195×10^{-6}	8.615×10^{4}	30 °C, 100% RH 2M CH_3OH	[86]
PSAAM-PMA	1.36×10^{-6}	/	30 °C, 100% RH	[87]
PSASB-PMA	1.61×10^{-6}	/	30 °C, 100% RH	[87]

RH—room temperature; M—molar concentration; RT—room temperature.

Table 3. List of achieved maximum power densities of biopolymer membranes and reference Nafion membranes tested in a single PEM fuel cell.

Polymer Type	Fuels	Addition or Filler	Max. Power Density [mW/cm^2]	Operating Conditions	Ref.
Chitosan	H_2/O_2	5 wt% of functionalised multi-walled carbon nanotubes (N-MWCNTs)	49.75	50 °C, 100% RH	[40]
Chitosan	2M CH_3OH/O_2	3 wt% of sulfonated polyaniline (PAni) and silicon dioxide (SiO_2)	56.27	80 °C, 100% RH	[43]
Chitosan	2M CH_3OH/O_2	4 wt% of phosphotungstic acid (PTA) immobilised on one-dimensional attapulgite (AT)	70.26	70 °C, 100% RH	[48]
Chitosan	2M CH_3OH/O_2	/	40.08	70 °C, 100% RH	[48]
Nafion 212	2M CH_3OH/O_2	/	79.87	70 °C, 100% RH	[48]
Chitosan	1M CH_3OH/O_2	Cross-linked for 30 s with HPA and then functionalised in a PTA/water solution for 24 h	60	70 °C 100% RH	[49]
Chitosan	H_2/O_2	Cross-linked for 30 s with STA and then functionalised in STA/water solution for 24 h	370	25 °C, 100% RH	[50]
Chitosan	2M CH_3OH/O_2	10 wt% of SO_3H-UiO-66 deposited on the surface of halloysite nanotubules (HNTs)	84.5	70 °C, 100% RH	[57]
Chitosan	2M CH_3OH/O_2	/	50.2	70 °C, 100% RH	[57]
Nafion 115	2M CH_3OH/O_2	/	92.4	70 °C, 100% RH	[57]
Chitosan	2M CH_3OH/O_2	1.5 wt% of MWCNTs and 0.05 mL of IL were added to the mixture of CS and PVA in the ratio of 10:90	82	70 °C, 100% RH	[60]
Nafion and cellulose	1M CH_3OH/air	Multilayer membrane NR211/CNC/NR212/ NR212	75.53	70 °C, 100% RH	[64]
Cellulose and PVDF	1M CH_3OH/O_2	The ratio of CNC and PVDF was 1:1, while the concentration of sulphuric acid during hydrolysis was 50%	8.65	25 °C, 100% RH	[66]
Nafion 117	1M CH_3OH/air	/	19	25 °C, 100% RH	[66]

Table 3. *Cont.*

Polymer Type	Fuels	Addition or Filler	Max. Power Density [mW/cm^2]	Operating Conditions	Ref.
Cellulose	H_2/O_2 H_2/air	Mixture of citric and phosphoric acid and coating with RDP in the ratio Cellulose/RDP 2:1	34.3 16.1	60 °C, 100% RH	[68]
Cellulose	H_2/air	Sulfonated cellulose nanofibres (30 µm) Sulfonated cellulose nanofibres (8 µm)	4.1 156	80 °C, 95% RH	[71]
Cellulose	H_2/O_2	Cellulose nanofibres cross-linked with 0.300 mL of 1 M citric acid	27.7	80 °C, 100% RH	[72]
Cellulose	H_2/air	Bacterial cellulose modified with APTES	4.85	95 °C, 100% RH	[75]
Cellulose	H_2/air	Cellulose acetate with 0.8 wt% of graphene oxide	519	60 °C, 100% RH	[79]
Nafion 212	H_2/air	/	401	60 °C, 100% RH	[79]
Sodium alginate	4M CH_3OH/air	20 wt% of TiO_2 and cross-linked with glutaraldehyde and glycerol	14.53 19.13	30 °C, 100% RH 60 °C, 100% RH	[86]
Keratin	H_2/O_2 H_2/air	Mixed keratin amyloid fibres with glyoxylic acid, then heating treatment and immersion of the membranes in peracetic acid	25 20	55 °C, 100% RH 65 °C, 100% RH	[98]

RT—room temperature; M—molar concentration.

3. Conclusions

PEMFCs are a cornerstone technology for the transition to sustainable energy systems, enabling the direct conversion of hydrogen's chemical energy into clean, zero-emission electricity. Due to hydrogen's high energy density, purity, and compatibility with renewable energy sources, hydrogen fuel cells represent one of the most promising pathways towards decarbonising the energy and transport sectors.

A major challenge hindering the widespread commercialisation of PEMFCs is the high production cost of polymer membranes. This issue, along with increasingly stringent environmental regulations promoting eco-friendly materials, has generated significant interest in biopolymers as alternative membrane materials. Biopolymers offer considerable potential as sustainable and cost-effective substitutes for conventional petroleum-based membranes. Although most biopolymer membranes still fall short of Nafion in overall performance, ongoing research demonstrates steady progress through chemical modification, cross-linking, and the incorporation of inorganic fillers to enhance their physicochemical and electrochemical properties. It is important to note that the highest proton conductivity values reported in this review are largely associated with membranes based on synthetic polymers, in which biopolymers are incorporated primarily as additives.

A comprehensive review of the literature indicates that chitosan and cellulose are the most extensively studied biopolymers for PEMFC applications, whereas others, such as keratin, collagen, and starch, remain relatively underexplored. Furthermore, only a limited number of studies have evaluated biopolymer membranes under actual fuel cell operating conditions. Among those that have, testing has largely been done to obtain the polarisation curve, which is among the most important indicators of membrane performance. However, these membranes must also undergo durability testing to enable proper assessment of their chemical and mechanical stability within the fuel cell environment. Most studies focus primarily on proton conductivity, which is a key parameter, but one that is insufficient on its own to fully evaluate membrane performance. Notably, the substantial variability in reported conductivity values highlights the need for standardised testing protocols. To ensure consistent and reliable comparison across studies, it is recommended that researchers

evaluate their biopolymer membranes alongside a reference Nafion membrane under identical conditions. Additionally, the development of a unified experimental setup, with standardised materials, catalyst loadings, and measurement procedures, would enable direct comparison of results, facilitate the identification of the most promising materials, and accelerate progress towards the design of high-performance, sustainable biopolymer membranes for PEMFCs.

Author Contributions: B.Š. conceptualised the study, developed the methodology, conducted the investigation, and drafted the manuscript. A.B., N.A. and Ž.P. contributed through critical review, editing, and revision of the manuscript. All authors have read and agreed to the published version of the manuscript.

Funding: The authors gratefully acknowledge funding from the Bilateral Ministry of Science and Technology, Israel (grant number: 1001703993) and the Ministry of Science and Education of Croatia through its Energy research grant program.

Data Availability Statement: The data used in this study are reported in the paper's figures and tables.

Acknowledgments: The authors gratefully acknowledge the financial support provided by the project STIM-REI (Contract No. KK.01.1.1.01.0003), funded by the European Union through the European Regional Development Fund under Operational Programme Competitiveness and Cohesion 2014–2020 (KK.01.1.1.01). The authors also acknowledge financial support from the project "Overcoming the Technological Hurdles in the Incorporation of Biopolymers as Ion Exchange Membranes in Fuel Cell Applications".

Conflicts of Interest: The authors declare no conflicts of interest.

Abbreviations

The following abbreviations are used in this manuscript:

$(C_6H_{10}O_5)_n$	Cellulose
AMPS	2-acrylamido-2-methyl-1-propanesulfonic acid
AT	Attapulgite
ATMP	Aminotris(methylenephosphonic acid)
BC	Bacterial cellulose
CA	Cellulose acetate
CNC	Nanocrystalline cellulose
CNF	Cellulose nanofibres
CNT	Carbon nanotube
CO_2	Carbon dioxide
CS	Chitosan
DMFC	Direct methanol fuel cell
DS	Degree of substitution
EIS	Electrochemical impedance spectroscopy
GA	Glutaraldehyde
GO	Graphene oxide
HNT	Halloysite nanotube
HPA	Heteropoly acid
IEC	Ion exchange capacity
IEMFC	Ion exchange membrane fuel cell
IL	Ionic liquid
Im	Imidazole
KOH	Potassium hydroxide
M	Molar concentration, (mol/L)
MCC	Microcrystalline cellulose
MEA	Membrane–electrode assembly

MOF	Metal–organic framework
MWCNT	Multi-walled carbon nanotube
NH_2	Amino group
NH_4SCN	Ammonium thiocyanate
OH	Hydroxyl group
OPA	Ortho-phosphoric acid
Pani	Polyaniline
PCS	Phosphorylated chitosan
PEG	Poly(ethylene glycol)
PEM	Proton exchange membrane
PEMFC	Proton exchange membrane fuel cell
PEO	Polyethylene oxide
PGO	Phosphorylated graphene oxide
Ph-CA	Phosphorylated cellulose acetate
PMA	Phosphomolybdic acid
PO_3H_2	Phosphoric acid group
PTA	Phosphotungstic acid
PVA	Polyvinyl alcohol
PVDF	Poly (vinylidene fluoride)
RDP	Resorcinol bis(diphenyl phosphate)
RH	Relative humidity
RT	Room temperature
SA	Sodium alginate
sChW	Sulfonated chitin nanofibre
s-CS	Sulfonated chitosan
SEM	Scanning electron microscope
s-GO	Sulfonated graphene oxide
SHS	Sodium hydrogen sulphate
SiO_2	Silicon oxide (silica)
SiWA	Silicotungstic acid
SO_3H	Sulfonic acid group
SPEEK	Sulfonated poly (ether ether ketone)
SVBS	Sodium 4-vinylbenzenesulfonate
SWCNT	Single-walled carbon nanotubes
TiO_2	Titanium dioxide
ZrO_2	Zirconium dioxide

References

1. Stephens, E.; Ross, I.L.; Mussgnug, J.H.; Wagner, L.D.; Borowitzka, M.A.; Posten, C.; Kruse, O.; Hankamer, B. Future prospects of microalgal biofuel production systems. *Trends Plant Sci.* **2010**, *15*, 554–564. [CrossRef]
2. Kumar, A.; Singh, P.; Raizada, P.; Hussain, C.M. Impact of COVID-19 on greenhouse gases emissions: A critical review. *Sci. Total. Environ.* **2022**, *806*, 150349. [CrossRef]
3. Bhukya, M.N.; Kumar, M.; Kant, A.; Punit. Renewable Energy: Potential, Status, Targets and Challenges in Rajasthan. *J. Phys. Conf. Ser.* **2021**, *1854*, 12004. [CrossRef]
4. Li, X.; Ye, T.; Meng, X.; He, D.; Li, L.; Song, K.; Jiang, J.; Sun, C. Advances in the Application of Sulfonated Poly(Ether Ether Ketone) (SPEEK) and Its Organic Composite Membranes for Proton Exchange Membrane Fuel Cells (PEMFCs). *Polymers* **2024**, *16*, 2840. [CrossRef]
5. Sadhasivam, T.; Kim, H.-T.; Jung, S.; Roh, S.-H.; Park, J.-H.; Jung, H.-Y. Dimensional effects of nanostructured Mg/MgH2 for hydrogen storage applications: A review. *Renew. Sustain. Energy Rev.* **2017**, *72*, 523–534. [CrossRef]
6. Gagliardi, G.G.; Ibrahim, A.; Borello, D.; El-Kharouf, A. Composite Polymers Development and Application for Polymer Electrolyte Membrane Technologies—A Review. *Molecules* **2020**, *25*, 1712. [CrossRef]
7. Cullen, D.A.; Neyerlin, K.C.; Ahluwalia, R.K.; Mukundan, R.; More, K.L.; Borup, R.L.; Weber, A.Z.; Myers, D.J.; Kusoglu, A. New roads and challenges for fuel cells in heavy-duty transportation. *Nat. Energy* **2021**, *6*, 462–474. [CrossRef]

8. Baroutaji, A.; Arjunan, A.; Robinson, J.; Wilberforce, T.; Abdelkareem, M.A.; Olabi, A.G. PEMFC Poly-Generation Systems: Developments, Merits, and Challenges. *Sustainability* **2021**, *13*, 11696. [CrossRef]
9. Meng, X.; Mei, J.; Tang, X.; Jiang, J.; Sun, C.; Song, K. The Degradation Prediction of Proton Exchange Membrane Fuel Cell Performance Based on a Transformer Model. *Energies* **2024**, *17*, 3050. [CrossRef]
10. Mahato, N.; Jang, H.; Dhyani, A.; Cho, S. Recent Progress in Conducting Polymers for Hydrogen Storage and Fuel Cell Applications. *Polymers* **2020**, *12*, 2480. [CrossRef] [PubMed]
11. Lufrano, E.; Simari, C.; Di Vona, M.L.; Nicotera, I.; Narducci, R. How the Morphology of Nafion-Based Membranes Affects Proton Transport. *Polymers* **2021**, *13*, 359. [CrossRef]
12. Meng, G.; Li, X.; Liu, M.; Grigoriev, S.A.; Tolj, I.; Shen, J.; Yue, C.; Sun, C. Investigations of Dongyue Series Perfluorosulfonic Acid Membranes for Applications in Proton Exchange Membrane Fuel Cells (PEMFCs). *Batteries* **2025**, *11*, 277. [CrossRef]
13. Auras, R.; Harte, B.; Selke, S. An Overview of Polylactides as Packaging Materials. *Macromol. Biosci.* **2004**, *4*, 835–864. [CrossRef] [PubMed]
14. Wang, S.; Lu, A.; Zhang, L. Recent advances in regenerated cellulose materials. *Prog. Polym. Sci.* **2016**, *53*, 169–206. [CrossRef]
15. Shaari, N.; Kamarudin, S. Chitosan and alginate types of bio-membrane in fuel cell application: An overview. *J. Power Sources* **2015**, *289*, 71–80. [CrossRef]
16. Samaniego, A.J.; Espiritu, R. Prospects on utilization of biopolymer materials for ion exchange membranes in fuel cells. *Green Chem. Lett. Rev.* **2022**, *15*, 253–275. [CrossRef]
17. Chibac-Scutaru, A.L.; Coseri, S. Advances in the use of cellulose-based proton exchange membranes in fuel cell technology: A review. *Int. J. Biol. Macromol.* **2023**, *247*, 125810. [CrossRef]
18. Doobi, F.A.; Mir, F.Q. Exploring the development of natural biopolymer (chitosan)-based proton exchange membranes for fuel cells: A review. *Results Surf. Interfaces* **2024**, *15*, 100218. [CrossRef]
19. Abouricha, S.; Aziam, H.; Noukrati, H.; Sel, O.; Saadoune, I.; Lahcini, M.; Ben Youcef, H. Biopolymers-Based Proton Exchange Membranes For Fuel Cell Applications: A Comprehensive Review. *ChemElectroChem* **2024**, *11*, e202300648. [CrossRef]
20. Barbir, F. *PEM Fuel Cells: Theory and Practice*, 2nd ed.; Academic Press: Amsterdam, The Netherlands, 2013.
21. Song, Y.; Guo, Z.; Yin, J.; Liu, M.; Tolj, I.; Grigoriev, S.A.; Ge, M.; Sun, C. Investigations of the Sulfonated Poly(ether ether ketone) Membranes with Various Degrees of Sulfonation by Considering Durability for the Proton Exchange Membrane Fuel Cell (PEMFC) Applications. *Polymers* **2025**, *17*, 2181. [CrossRef] [PubMed]
22. Kusoglu, A.; Weber, A.Z. New Insights into Perfluorinated Sulfonic-Acid Ionomers. *Chem. Rev.* **2017**, *117*, 987–1104. [CrossRef] [PubMed]
23. Lim, D.-W.; Sadakiyo, M.; Kitagawa, H. Proton transfer in hydrogen-bonded degenerate systems of water and ammonia in metal–organic frameworks. *Chem. Sci.* **2019**, *10*, 16–33. [CrossRef]
24. Li, Z.; Yao, Y.; Wang, D.; Hasan, M.; Suwansoontorn, A.; Li, H.; Du, G.; Liu, Z.; Nagao, Y. Simple and universal synthesis of sulfonated porous organic polymers with high proton conductivity. *Mater. Chem. Front.* **2020**, *4*, 2339–2345. [CrossRef]
25. Zhu, L.-Y.; Li, Y.-C.; Liu, J.; He, J.; Wang, L.-Y.; Lei, J.-D. Recent developments in high-performance Nafion membranes for hydrogen fuel cells applications. *Pet. Sci.* **2022**, *19*, 1371–1381. [CrossRef]
26. Amir Qureshi, M. An Overview on Wounds Their Issues and Natural Remedies for Wound Healing. *Biochem. Physiol. Open Access* **2015**, *4*, 1000165. [CrossRef]
27. Schaffer, J.V.; Lupatini, K.N.; Machado, B.; Silva, E.S.; Ferracin, R.J.; Alves, H.J. Parameters effect on proton conductivity to obtain chitosan membranes for use as electrolytes in PEMFC. *Int. J. Energy Res.* **2018**, *42*, 1381–1385. [CrossRef]
28. Liu, H.; Gong, C.; Wang, J.; Liu, X.; Liu, H.; Cheng, F.; Wang, G.; Zheng, G.; Qin, C.; Wen, S. Chitosan/silica coated carbon nanotubes composite proton exchange membranes for fuel cell applications. *Carbohydr. Polym.* **2016**, *136*, 1379–1385. [CrossRef]
29. Chakrabarty, T.; Kumar, M.; Shahi, V.K. Chitosan Based Membranes for Separation, Pervaporation and Fuel Cell Applications: Recent Developments. In *Biopolymers*; Elnashar, M., Ed.; IntechOpen: Rijeka, Croatia, 2010; Chapter 10. [CrossRef]
30. Dimassi, S.; Tabary, N.; Chai, F.; Blanchemain, N.; Martel, B. Sulfonated and sulfated chitosan derivatives for biomedical applications: A review. *Carbohydr. Polym.* **2018**, *202*, 382–396. [CrossRef]
31. Tan, W.; Zhang, J.; Zhao, X.; Dong, F.; Li, Q.; Guo, Z. Synthesis and antioxidant action of chitosan derivatives with amino-containing groups via azide-alkyne click reaction and N-methylation. *Carbohydr. Polym.* **2018**, *199*, 583–592. [CrossRef]
32. Kalaiselvimary, J.; Prabhu, M.R. Influence of sulfonated GO/sulfonated biopolymer as polymer electrolyte membrane for fuel cell application. *J. Mater. Sci. Mater. Electron.* **2018**, *29*, 5525–5535. [CrossRef]
33. Nasirinezhad, M.; Ghaffarian, S.R.; Tohidian, M. Eco-friendly polyelectrolyte nanocomposite membranes based on chitosan and sulfonated chitin nanowhiskers for fuel cell applications. *Iran. Polym. J.* **2021**, *30*, 355–367. [CrossRef]
34. Wu, H.; Hou, W.; Wang, J.; Xiao, L.; Jiang, Z. Preparation and properties of hybrid direct methanol fuel cell membranes by embedding organophosphorylated titania submicrospheres into a chitosan polymer matrix. *J. Power Sources* **2010**, *195*, 4104–4113. [CrossRef]

35. Zeng, J.; He, B.; Lamb, K.; De Marco, R.; Shen, P.K.; Jiang, S.P. Phosphoric acid functionalized pre-sintered meso-silica for high temperature proton exchange membrane fuel cells. *Chem. Commun.* **2013**, *49*, 4655–4657. [CrossRef] [PubMed]
36. Itoh, T.; Hirai, K.; Tamura, M.; Uno, T.; Kubo, M.; Aihara, Y. Anhydrous proton-conducting electrolyte membranes based on hyperbranched polymer with phosphonic acid groups for high-temperature fuel cells. *J. Power Sources* **2008**, *178*, 627–633. [CrossRef]
37. Jung, G.-B.; Tseng, C.-C.; Yeh, C.-C.; Lin, C.-Y. Membrane electrode assemblies doped with H3PO4 for high temperature proton exchange membrane fuel cells. *Int. J. Hydrogen Energy* **2012**, *37*, 13645–13651. [CrossRef]
38. Nores-Pondal, F.J.; Buera, M.P.; Corti, H.R. Thermal properties of phosphoric acid-doped polybenzimidazole membranes in water and methanol–water mixtures. *J. Power Sources* **2010**, *195*, 6389–6397. [CrossRef]
39. Ahmed, S.; Cai, Y.; Ali, M.; Khannal, S.; Ahmad, Z.; Lu, Y.; Wang, S.; Xu, S. One-step phosphorylation of graphene oxide for the fabrication of nanocomposite membranes with enhanced proton conductivity for fuel cell applications. *J. Mater. Sci. Mater. Electron.* **2019**, *30*, 13056–13066. [CrossRef]
40. Ahmed, S.; Tao, Z.; Zhang, H.; Ahmed, N.; Gulzar, H.; Wang, J. Tuning the Performance of Nanofiller Reinforced Phosphorylated Chitosan-Based Proton Exchange Membrane. *J. Electrochem. Soc.* **2023**, *170*, 024501. [CrossRef]
41. Pokprasert, A.; Chirachanchai, S. Proton conductivity and dimensional stability of proton exchange membrane: A dilemma solved by chitosan aerogel framework. *Electrochim. Acta* **2023**, *441*, 141764. [CrossRef]
42. Handika, G.; Ghozali, A.I.; Saga, B.H. Synthesis and Characterization of Electrolyte Membrane Based Biopolymer Chitosan and Fly Ash Combinations for Fuel Cell Application. In *Seminar Nasional Kimia-National Seminar on Chemistry (SNK 2018)*; Atlantis Press: Dordrecht, The Netherlands, 2018; pp. 95–98.
43. Vijayakumar, V.; Khastgir, D. Hybrid composite membranes of chitosan/sulfonated polyaniline/silica as polymer electrolyte membrane for fuel cells. *Carbohydr. Polym.* **2018**, *179*, 152–163. [CrossRef] [PubMed]
44. Cui, F.; Wang, W.-Y.; Shan, B.; Liu, C.; Xie, C.; Zhu, L.; Chen, X.; Li, N. Enhanced Performance of the Chitosan Proton Exchange Membrane via Anatase Titania Anchored GO and Sodium Ligninsulfonate Constructing Proton Transport Channels. *Energy Fuels* **2020**, *34*, 3867–3876. [CrossRef]
45. Cavallaro, G.; Micciulla, S.; Chiappisi, L.; Lazzara, G. Chitosan-based smart hybrid materials: A physico-chemical perspective. *J. Mater. Chem. B* **2021**, *9*, 594–611. [CrossRef] [PubMed]
46. Nimir, W.; Al-Othman, A.; Tawalbeh, M.; Al Makky, A.; Ali, A.; Karimi-Maleh, H.; Karimi, F.; Karaman, C. Approaches towards the development of heteropolyacid-based high temperature membranes for PEM fuel cells. *Int. J. Hydrogen Energy* **2023**, *48*, 6638–6656. [CrossRef]
47. Spasov, D.D.; Mensharapov, R.M.; Sinyakov, M.V.; Grineva, D.E.; Ivanova, N.A.; Li, X.; Sun, C.; Kulikov, L.A.; Makeeva, D.A.; Grigoriev, S.A. Polybenzimidazole Membranes Modified with Porous Aromatic Frameworks: Synthesis, Structure, Mechanical and Transport Properties. *Nanoenergy Adv.* **2026**, *6*, 3. [CrossRef]
48. Tsen, W.-C. Composite Proton Exchange Membranes Based on Chitosan and Phosphotungstic Acid Immobilized One-Dimensional Attapulgite for Direct Methanol Fuel Cells. *Nanomaterials* **2020**, *10*, 1641. [CrossRef]
49. Zaffora, A.; Di Franco, F.; Gradino, E.; Santamaria, M. Methanol and proton transport through chitosan-phosphotungstic acid membranes for direct methanol fuel cell. *Int. J. Energy Res.* **2020**, *44*, 11550–11563. [CrossRef]
50. Di Franco, F.; Zaffora, A.; Burgio, G.; Santamaria, M. Performance of H2-fed fuel cell with chitosan/silicotungstic acid membrane as proton conductor. *J. Appl. Electrochem.* **2020**, *50*, 333–341. [CrossRef]
51. Mahmodi, G.; Zarrintaj, P.; Taghizadeh, A.; Taghizadeh, M.; Manouchehri, S.; Dangwal, S.; Ronte, A.; Ganjali, M.R.; Ramsey, J.D.; Kim, S.-J.; et al. From microporous to mesoporous mineral frameworks: An alliance between zeolite and chitosan. *Carbohydr. Res.* **2020**, *489*, 107930. [CrossRef]
52. Wu, H.; Zheng, B.; Zheng, X.; Wang, J.; Yuan, W.; Jiang, Z. Surface-modified Y zeolite-filled chitosan membrane for direct methanol fuel cell. *J. Power Sources* **2007**, *173*, 842–852. [CrossRef]
53. Shang, J.; Zhong, S.; Zhao, Y.; Wang, B.; Gao, Y.; Xiang, W.; Cui, X. Preparation of chitosan-modified core–shell SiO_2-acidic polymer multiple crosslinked membranes. *J. Appl. Polym. Sci.* **2020**, *137*, 48494. [CrossRef]
54. Gómez, E.E.R.; Hernández, J.H.M.; Astaiza, J.E.D. Development of a Chitosan/PVA/TiO_2 Nanocomposite for Application as a Solid Polymeric Electrolyte in Fuel Cells. *Polymers* **2020**, *12*, 1691. [CrossRef]
55. Li, X.; Gao, J. Recent advances of metal–organic frameworks-based proton exchange membranes in fuel cell applications. *Susmat* **2022**, *2*, 504–534. [CrossRef]
56. Wang, J.; Gong, C.; Wen, S.; Liu, H.; Qin, C.; Xiong, C.; Dong, L. Proton exchange membrane based on chitosan and solvent-free carbon nanotube fluids for fuel cells applications. *Carbohydr. Polym.* **2018**, *186*, 200–207. [CrossRef] [PubMed]
57. Zhao, S.; Yang, Y.; Zhong, F.; Niu, W.; Liu, Y.; Zheng, G.; Liu, H.; Wang, J.; Xiao, Z. Fabrication of composite polymer electrolyte membrane using acidic metal-organic frameworks-functionalized halloysite nanotubes modified chitosan. *Polymer* **2021**, *226*, 123800. [CrossRef]

58. Nurazzi, N.M.; Sabaruddin, F.A.; Harussani, M.M.; Kamarudin, S.H.; Rayung, M.; Asyraf, M.R.M.; Aisyah, H.A.; Norrrahim, M.N.F.; Ilyas, R.A.; Abdullah, N.; et al. Mechanical Performance and Applications of CNTs Reinforced Polymer Composites—A Review. *Nanomaterials* **2021**, *11*, 2186. [CrossRef]
59. Ahmed, S.; Ali, M.; Cai, Y.; Lu, Y.; Ahmad, Z.; Khannal, S.; Xu, S. Novel sulfonated multi-walled carbon nanotubes filled chitosan composite membrane for fuel-cell applications. *J. Appl. Polym. Sci.* **2019**, *136*, 47603. [CrossRef]
60. Murmu, R.; Roy, D.; Jena, S.; Sutar, H. Development of chitosan-based hybrid membrane modified with ionic-liquid and carbon nanotubes for direct methanol fuel cell operating at moderate temperature. *Polym. Bull.* **2023**, *80*, 3949–3980. [CrossRef]
61. Trache, D.; Tarchoun, A.F.; Derradji, M.; Hamidon, T.S.; Masruchin, N.; Brosse, N.; Hussin, M.H. Nanocellulose: From Fundamentals to Advanced Applications. *Front. Chem.* **2020**, *8*, 392. [CrossRef]
62. He, X.; Lu, W.; Sun, C.; Khalesi, H.; Mata, A.; Andaleeb, R.; Fang, Y. Cellulose and cellulose derivatives: Different colloidal states and food-related applications. *Carbohydr. Polym.* **2021**, *255*, 117334. [CrossRef]
63. Ni, C.; Wei, Y.; Hu, Q.; Li, X.; Liu, B.; Zhao, Q.; Zhang, M.; Li, Y.; Hu, W. Nanocystalline cellulose reinforced sulfonated fluorenyl-containing polyaryletherketones for proton exchange membranes. *Solid State Ion.* **2016**, *297*, 29–35. [CrossRef]
64. Hosseinpour, M.; Sahoo, M.; Perez-Page, M.; Baylis, S.R.; Patel, F.; Holmes, S.M. Improving the performance of direct methanol fuel cells by implementing multilayer membranes blended with cellulose nanocrystals. *Int. J. Hydrogen Energy* **2019**, *44*, 30409–30419. [CrossRef]
65. Pambudi, A.B.; Priyangga, A.; Hartanto, D.; Atmaja, L. Fabrication and characterization of modified microcrystalline cellulose membrane as proton exchange membrane for direct methanol fuel cell. *Mater. Today Proc.* **2020**, *46*, 1855–1859. [CrossRef]
66. Muhmed, S.; Jaafar, J.; Daud, S.; Hanifah, M.F.R.; Purwanto, M.; Othman, M.; Rahman, M.; Ismail, A. Improvement in properties of nanocrystalline cellulose/poly (vinylidene fluoride) nanocomposite membrane for direct methanol fuel cell application. *J. Environ. Chem. Eng.* **2021**, *9*, 105577. [CrossRef]
67. Ben Moussa, M.A.; Ahmed, Z.; Charradi, K.; Ben Fraj, B.; Boufi, S.; Koschella, A.; Heinze, T.; Keshk, S.M.A.S.; Ben Assaker, I. Performance of high sulfonated poly(ether ether ketone) improved with microcrystalline cellulose and 2,3-dialdehyde cellulose for proton exchange membranes. *Mater. Renew. Sustain. Energy* **2024**, *13*, 319–331. [CrossRef]
68. Raut, A.; Fang, H.; Lin, Y.-C.; Rahman, F.; Fu, S.; Yin, Y.; Fang, Y.; Sprouster, D.; Isseroff, R.; Sharma, S.K.; et al. Designing a micro-cellulose membrane for hydrogen fuel cells. *RSC Sustain.* **2025**, *3*, 3025–3035. [CrossRef]
69. Thomas, S.; Pottathara, Y.B. *Nanocellulose Based Composites for Electronics*; Elsevier Inc.: Amsterdam, The Netherlands, 2020. [CrossRef]
70. Hsieh, Y.-L. Cellulose Nanofibers: Electrospinning and Nanocellulose Self-Assemblies. 2018. Available online: https://escholarship.org/uc/item/4rq8b8t1 (accessed on 13 May 2026).
71. Bayer, T.; Cunning, B.V.; Šmíd, B.; Selyanchyn, R.; Fujikawa, S.; Sasaki, K.; Lyth, S.M. Spray deposition of sulfonated cellulose nanofibers as electrolyte membranes in fuel cells. *Cellulose* **2021**, *28*, 1355–1367. [CrossRef]
72. Li, S.; Cai, G.; Wu, S.; Raut, A.; Borges, W.; Sharma, P.R.; Sharma, S.K.; Hsiao, B.S.; Rafailovich, M. Sustainable Plant-Based Biopolymer Membranes for PEM Fuel Cells. *Int. J. Mol. Sci.* **2022**, *23*, 15245. [CrossRef] [PubMed]
73. Zhong, C. Industrial-Scale Production and Applications of Bacterial Cellulose. *Front. Bioeng. Biotechnol.* **2020**, *8*, 605374. [CrossRef]
74. Gregory, D.A.; Tripathi, L.; Fricker, A.T.; Asare, E.; Orlando, I.; Raghavendran, V.; Roy, I. Bacterial cellulose: A smart biomaterial with diverse applications. *Mater. Sci. Eng. R Rep.* **2021**, *145*, 100623. [CrossRef]
75. Yang, X.; Huang, L.; Deng, Q.; Dong, W. A Sustainable and Eco-Friendly Membrane for PEM Fuel Cells Using Bacterial Cellulose. *Polymers* **2024**, *16*, 3017. [CrossRef]
76. Fei, P.; Liao, L.; Cheng, B.; Song, J. Quantitative analysis of cellulose acetate with a high degree of substitution by FTIR and its application. *Anal. Methods* **2017**, *9*, 6194–6201. [CrossRef]
77. Beek, P.; Koelemeijer, K.; Zuilichem, D.J.; Reinders, M.P.; Meffert, H.F.T. Encyclopedia of food sciences and nutrition. In *Transport Logistics of Food*; Academic Press: San Diego, CA, USA, 2003; pp. 5835–5851.
78. Khalifa, R.E.; Omer, A.M.; Elmageed, M.H.A.; Eldin, M.S.M. Titanium Dioxide/Phosphorous-Functionalized Cellulose Acetate Nanocomposite Membranes for DMFC Applications: Enhancing Properties and Performance. *ACS Omega* **2021**, *6*, 17194–17202. [CrossRef] [PubMed]
79. Madih, K.; El-Shazly, A.; Elkady, M.; Aziz, A.N.; Youssef, M.E.; Khalifa, R.E. A facile synthesis of cellulose acetate reinforced graphene oxide nanosheets as proton exchange membranes for fuel cell applications. *J. Saudi Chem. Soc.* **2022**, *26*, 101435. [CrossRef]
80. Khalaf, M.; Saeed, A.M.; Ali, A.I.; Kamoun, E.A.; Fahmy, A. Polyelectrolyte membranes based on phosphorylated-PVA/cellulose acetate for direct methanol fuel cell applications: Synthesis, instrumental characterization, and performance testing. *Sci. Rep.* **2023**, *13*, 13011. [CrossRef] [PubMed]
81. Ramaiah, S.; Kumar, T.M.P.; Ravi, V. Studies on Biopolymers for Ophthalmic Drug Delivery. *J. Macromol. Sci. Part A* **2007**, *44*, 229–234. [CrossRef]
82. Shah, J.; Jani, D.; Parikh, J. Gellan Gum and Its Applications—A Review. *Pharm. Rev.* **2007**.

83. Naachiyar, R.M.; Ragam, M.; Selvasekarapandian, S.; Krishna, M.V.; Buvaneshwari, P. Development of biopolymer electrolyte membrane using Gellan gum biopolymer incorporated with NH4SCN for electro-chemical application. *Ionics* **2021**, *27*, 3415–3429. [CrossRef]
84. Eswaramma, S.; Rao, K.K. Synthesis of dual responsive carbohydrate polymer based IPN microbeads for controlled release of anti-HIV drug. *Carbohydr. Polym.* **2017**, *156*, 125–134. [CrossRef] [PubMed]
85. Jabeen, S.; Chat, O.A.; Maswal, M.; Ashraf, U.; Rather, G.M.; Dar, A.A. Hydrogels of sodium alginate in cationic surfactants: Surfactant dependent modulation of encapsulation/release toward Ibuprofen. *Carbohydr. Polym.* **2015**, *133*, 144–153. [CrossRef]
86. Shaari, N.; Kamarudin, S.K.; Zakaria, Z. Potential of sodium alginate/titanium oxide biomembrane nanocomposite in DMFC application. *Int. J. Energy Res.* **2019**, *43*, 8057–8069. [CrossRef]
87. Vijitha, R.; Nagaraja, K.; Hanafiah, M.M.; Rao, K.M.; Venkateswarlu, K.; Lakkaboyana, S.K.; Rao, K.S.V.K. Fabrication of Eco-Friendly Polyelectrolyte Membranes Based on Sulfonate Grafted Sodium Alginate for Drug Delivery, Toxic Metal Ion Removal and Fuel Cell Applications. *Polymers* **2021**, *13*, 3293. [CrossRef] [PubMed]
88. Yusoff, Y.N.; Shaari, N.; A Mohamed, M.; Loh, K.S.; Kamarudin, S.K. Enhanced proton conductivity and mechanical stability of crosslinked sodium alginate as a biopolymer electrolyte membrane in fuel cell application. *IOP Conf. Ser. Earth Environ. Sci.* **2024**, *1372*, 012104. [CrossRef]
89. Bhuniya, S.; Demina, T.S.; Akopova, T.A. Advances in Applications of Polysaccharides and Polysaccharide-Based Materials. *Int. J. Mol. Sci.* **2024**, *25*, 6482. [CrossRef]
90. Ding, J.; Yang, Y.; Poisson, J.; He, Y.; Zhang, H.; Zhang, Y.; Bao, Y.; Chen, S.; Chen, Y.M.; Zhang, K. Recent Advances in Biopolymer-Based Hydrogel Electrolytes for Flexible Supercapacitors. *ACS Energy Lett.* **2024**, *9*, 1803–1825. [CrossRef] [PubMed]
91. Chauhan, J.K.; Kumar, M.; Yadav, M.; Tiwari, T.; Srivastava, N. Effect of NaClO4 concentration on electrolytic behaviour of corn starch film for supercapacitor application. *Ionics* **2017**, *23*, 2943–2949. [CrossRef]
92. Al-Othman, A.; Tawalbeh, M.; Ka'Ki, A.; Mohamad, S.; Hassan, M.F.; Almomani, F. Strach/Chitosan Membranes for PEM Fuel Cells Applications. In Proceedings of the 2023 Advances in Science and Engineering Technology International Conferences, Dubai, United Arab Emirates, 20–23 February 2023. [CrossRef]
93. Hassan, M.F.; Johar, M.I.; Zahari, M.Z.M.; Sheng, C.K. Utilizing sodium salt complexed with biopolymer as ionic-conducting electrolyte membrane: A study of morphology, structure and ionic conductivity. *Bull. Mater. Sci.* **2025**, *48*, 59. [CrossRef]
94. Feroz, S.; Muhammad, N.; Ratnayake, J.; Dias, G. Keratin-Based materials for biomedical applications. *Bioact. Mater.* **2020**, *5*, 496–509. [CrossRef]
95. Hill, P.; Brantley, H.; Van Dyke, M. Some properties of keratin biomaterials: Kerateines. *Biomaterials* **2010**, *31*, 585–593. [CrossRef]
96. Wang, B.; Yang, W.; McKittrick, J.; Meyers, M.A. Keratin: Structure, mechanical properties, occurrence in biological organisms, and efforts at bioinspiration. *Prog. Mater. Sci.* **2016**, *76*, 229–318. [CrossRef]
97. Sinha, P.; Yadav, A.; Tyagi, A.; Paik, P.; Yokoi, H.; Naskar, A.K.; Kuila, T.; Kar, K.K. Keratin-derived functional carbon with superior charge storage and transport for high-performance supercapacitors. *Carbon* **2020**, *168*, 419–438. [CrossRef]
98. Soon, W.L.; Peydayesh, M.; de Wild, T.; Donat, F.; Saran, R.; Müller, C.R.; Gubler, L.; Mezzenga, R.; Miserez, A. Renewable Energy from Livestock Waste Valorization: Amyloid-Based Feather Keratin Fuel Cells. *ACS Appl. Mater. Interfaces* **2023**, *15*, 47049–47057. [CrossRef] [PubMed]
99. Gustian, I.; Simalango, A.; Triawan, D.A.; Putranto, A.M.H.; Asdim. Synthesis and characterization of proton-conducting membranes based on bacterial cellulose and human nail keratin. *e-Polymers* **2023**, *23*, 20230040. [CrossRef]
100. Lo, S.; Fauzi, M.B. Current Update of Collagen Nanomaterials—Fabrication, Characterisation and Its Applications: A Review. *Pharmaceutics* **2021**, *13*, 316. [CrossRef]
101. Bazrafshan, Z.; Stylios, G.K. Spinnability of collagen as a biomimetic material: A review. *Int. J. Biol. Macromol.* **2019**, *129*, 693–705. [CrossRef]
102. Lei, J.; Zhou, J.; Li, J.; Wen, J.; Su, L.; Duan, T.; Zhu, W. Novel collagen waste derived Mn-doped nitrogen-containing carbon for supercapacitors. *Electrochimica Acta* **2018**, *285*, 292–300. [CrossRef]
103. Mekonnen, B.T.; Meiyazhagan, A.; Ragothaman, M.; Kalirajan, C.; Palanisamy, T. Bi-functional iron embedded carbon nanostructures from collagen waste for photocatalysis and Li-ion battery applications: A waste to wealth approach. *J. Clean. Prod.* **2019**, *210*, 190–199. [CrossRef]
104. Matsui, H.; Matsuo, Y. Proton Conduction via Water Bridges Hydrated in the Collagen Film. *J. Funct. Biomater.* **2020**, *11*, 61. [CrossRef]
105. Orieshyna, A.; Puetzer, J.L.; Amdursky, N. Proton Transport Across Collagen Fibrils and Scaffolds: The Role of Hydroxyproline. *Biomacromolecules* **2023**, *24*, 4653–4662. [CrossRef]
106. Furuseki, T.; Teranishi, S.; Matsuo, Y. Study on Anhydrous Proton Conduction in Imidazole–Collagen Composite. *J. Compos. Sci.* **2022**, *6*, 360. [CrossRef]

107. Ali, A.A.; Al-Othman, A.; Tawalbeh, M.; Almomani, F. Collagen Based Biomaterials as Membranes for PEM Fuel Cells Applications. In Proceedings of the Advances in Science and Engineering Technology International Conferences, ASET, Dubai, United Arab Emirates, 26–29 February 2024. [CrossRef]
108. Foqara, M.; Nandi, R.; Amdursky, N. Casein proteins as building blocks for making ion-conductive bioplastics. *J. Mater. Chem. A* **2022**, *10*, 14529–14539. [CrossRef]
109. Yang, Z.; Sarkar, A.K.; Amdursky, N. Glycoproteins as a Platform for Making Proton-Conductive Free-Standing Biopolymers. *Biomacromolecules* **2023**, *24*, 1111–1120. [CrossRef] [PubMed]
110. Mondal, S.; Agam, Y.; Nandi, R.; Amdursky, N. Exploring long-range proton conduction, the conduction mechanism and inner hydration state of protein biopolymers. *Chem. Sci.* **2020**, *11*, 3547–3556. [CrossRef] [PubMed]
111. Agam, Y.; Nandi, R.; Bulava, T.; Amdursky, N. The role of the protein–water interface in dictating proton conduction across protein-based biopolymers. *Mater. Adv.* **2021**, *2*, 1739–1746. [CrossRef]
112. Mondal, S.; Agam, Y.; Amdursky, N. Proton Conductivity: Enhanced Proton Conductivity across Protein Biopolymers Mediated by Doped Carbon Nanoparticles (Small 50/2020). *Small* **2020**, *16*, 2070272. [CrossRef]
113. Nandi, R.; Agam, Y.; Amdursky, N. A Protein-Based Free-Standing Proton-Conducting Transparent Elastomer for Large-Scale Sensing Applications. *Adv. Mater.* **2021**, *33*, e2101208. [CrossRef] [PubMed]